Quadratic spline collocation for one-dimensional linear parabolic partial differential equations

Christina C. Christara, Tong Chen and Duy Minh Dang
Department of Computer Science, University of Toronto
Toronto, Ontario M5S 3G4, Canada
{ccc, tchen, dmdang}@cs.toronto.edu

Abstract

New methods for solving general linear parabolic partial differential equations (PDEs) in one space dimension are developed. The methods combine quadratic-spline collocation for the space discretization and classical finite differences, such as Crank-Nicolson, for the time discretization. The main computational requirements of the most efficient method are the solution of one tridiagonal linear system at each time step, while the resulting errors at the gridpoints and midpoints of the space partition are fourth order. The stability and convergence properties of some of the new methods are analyzed for a model problem. Numerical results demonstrate the stability and accuracy of the methods. Adaptive mesh techniques are introduced in the space dimension, and the resulting method is applied to the American put option pricing problem, giving very competitive results.

1 Introduction

Collocation is a simple to implement discretization technique for differential equations' problems that gives an approximation to the solution over the whole domain of the problem. Collocation assumes that the approximate solution to a differential equation problem belongs to an approximation space, often chosen to be a space of piecewise polynomials, with respect to a partition of the problem's domain. Given an interval and a node partition of the interval, splines are piecewise polynomials of a certain degree k and continuity $\mathcal{C}^{k-1}$ at the nodes of the partition, that is, they exhibit maximum smoothness. Spline collocation, that is, collocation using a spline space as approximation space, has been primarily used for the solution of Boundary Value Problems (BVPs) for ODEs or PDEs, and shown to be an effective method [14]. The standard formulation of spline collocation leads to sub-optimal order of convergence of the approximation to the solution. Two other types of spline collocation methods have been developed, the extrapolated (a.k.a. modified) and the deferred-correction methods, both giving rise to optimal order of convergence. These methods have been extended recently to non-uniform grids and integrated with adaptive techniques.

Orthogonal piecewise polynomial collocation was first introduced and analyzed in [8] for general two-point BVPs. In [8], the approximation space is a space of piecewise polynomials of degree at least three and continuity $\mathcal{C}^1$. We remark that orthogonal piecewise polynomial collocation is also referred to as spline collocation at the Gauss points, however, to avoid any confusion, in this paper we use the term "spline" to refer to maximum smoothness piecewise polynomials. Orthogonal piecewise polynomial collocation for parabolic PDEs in one space dimension has been studied in [9, 10]. Optimal orders of convergence, including superconvergence at the knots, have been shown for continuous and discrete time errors. The case of two space dimensions is studied in [12]. In [19, 18], orthogonal collocation is combined with adaptive mesh techniques and the method of lines to solve 1-D parabolic PDEs within specified accuracy. A comprehensive survey of orthogonal piecewise polynomial collocation methods for differential equations in one or more space dimensions (including elliptic, parabolic and hyperbolic) is found in [2], where a wealthy list of references is provided, and where a brief section on (fully smooth) spline collocation methods is included. Extrapolated cubic-spline collocation is formulated and analysed in [1], where optimal orders for continuous time errors (excluding superconvergence of the derivative) are obtained. In this paper, we consider quadratic-spline collocation methods for the space discretization of parabolic PDEs. We focus primarily on the case of one space dimension, but some of the results in this paper can be naturally extended to two or more dimensions. The time discretization is handled by finite difference techniques. There are two typical ways for introducing spline collocation for the space discretization of parabolic PDEs: (a) using spline collocation in its standard formulation, which has second-order accuracy, and requires the solution of one tridiagonal linear system at each time step; (b) using deferred-correction (two-step methods) or extrapolated (one-step methods) spline collocation, resulting in fourth-order accuracy at the midpoints and gridpoints of the partition, and requiring the solution of either two tridiagonal linear systems or an almost pentadiagonal linear system at each time step. By "almost pentadiagonal" we mean that all rows of the matrix, except the first two and last two rows, follow a pentadiagonal pattern. Yet another technique is introduced here, which gives rise to one-step, yet non-extrapolated methods, and has the advantages of the above two techniques: it gives fourth-order accuracy at the midpoints and gridpoints of the partition, and requires the solution of one tridiagonal linear system at each time step.

While this paper is not meant to provide a thorough review and comparison of orthogonal piecewise polynomial and spline collocation methods, we make a few relevant remarks. For a given partition size and degree piecewise polynomials, spline collocation gives rise to fewer unknowns than orthogonal piecewise polynomial collocation. However, orthogonal piecewise polynomial collocation has been developed for general degree piecewise polynomials and general order differential operators, while optimal spline collocation has been developed for low degree splines and more restricted differential operators. Furthermore, the formulation of optimal spline collocation methods on non-uniform grids is not as simple as that of orthogonal piecewise polynomial collocation. Moreover, it is worth making a few remarks regarding quadratic and cubic spline collocation. The accuracy of cubic splines is fourth order over the whole domain, while quadratic splines give fourth order only at the nodes and midpoints of a partition. However, cubic spline collocation is less straightforward to extend from one-dimensional to two-dimensional (or higher dimensional) problems. This is primarily due to the fact that cubic spline collocation for a two-point BVP usually collocates both the interior and the boundary differential operators at the boundary points, and in two dimensions the need for some extra corner conditions arises. Furthermore, quadratic splines are $\mathcal{C}^1$ and cubic splines are $\mathcal{C}^2$, and practitioners may, for various reasons, prefer one or the other.

In Section 2, we introduce the new methods. In Sections 3 and 4, we study the stability and convergence properties of certain extrapolated methods. In Section 5, we study the stability and convergence properties of certain one-step non-extrapolated methods, identify cases of instability, and propose stable improvements, without sacrificing accuracy and efficiency. In Section 6, we combine the new methods with adaptive techniques in the space dimension. These techniques maintain the same number of points at each timestep, but place the points in a way that results in a better error distribution along the spatial domain. Section 7, presents results that demonstrate the stability and convergence properties of the methods.We also apply the adaptive spline collocation methods to the American put option pricing problem, formulated as a free-boundary PDE problem. The numerical experiments indicate that the proposed method correctly captures the behaviour of the problem, including the discontinuities due to the initial conditions and the free boundary. We conclude in Section 8.

2 Problem and Discretization

We are concerned with the numerical solution of the parabolic PDE problem

$$\begin{aligned} u_t - \mathcal{L}u \quad &= g \qquad \text{in} \quad \Omega \times (0,T) && (1)\\ \mathcal{B}u \quad &= \gamma \qquad \text{on} \quad \partial\Omega \times (0,T) && (2)\\ u \quad &= u^0 \qquad \text{on} \quad (\partial\Omega \cup \Omega) \times \{0\}, && (3) \end{aligned}$$

where $\mathcal{L}u(x,t) \equiv p(x,t)u_{xx}(x,t) + q(x,t)u_x(x,t) + r(x,t)u(x,t)$ is a linear second-order operator, $\mathcal{B}u(x,t) \equiv \alpha(x,t)u(x,t) + \beta(x,t)u_x(x,t)$ a boundary operator, $p, q, r, g, \alpha, \beta, \gamma, u^0$ are given functions, $\Omega \equiv (\omega_a, \omega_b)$ is the spatial domain, $(0,T)$ with $T > 0$ is the time domain, and $u(x,t)$ is the unknown function. Thoughout the paper, we assume that $p(x,t) > 0$ and $|\alpha(x,t)| + |\beta(x,t)| > 0$.

We apply a standard Finite Difference (FD) discretization of (1) in the time dimension

$$(\mathcal{I} - \lambda h_t \mathcal{L}^j)U^j(x) = (\mathcal{I} + (1-\lambda)h_t\mathcal{L}^{j-1})U^{j-1}(x) + h_t(\lambda g^j(x) + (1-\lambda)g^{j-1}(x)),\ x \in \Omega, \qquad (4)$$

where $U^j(x) \equiv U(x, t_j)$ is the approximation to $u(x, t_j)$ at the jth time step, $g^j(x) \equiv g(x, t_j)$, and the superscript j in $\mathcal{L}^j$ denotes that the functions-coefficients p, q and r are evaluated at t_j. In general, the superscript j applied to an operator or function of t (and possibly x) denotes evaluation of the operator or function at t_j. If a uniform time stepsize h_t is chosen, then $t_j = jh_t$. The values $\lambda = 1/2$ and $\lambda = 1$ give rise to the standard Crank-Nicolson (CN) and fully-implicit methods, respectively. The above time-stepping technique, together with appropriate boundary conditions, can be viewed as equivalent to solving a BVP at each time step.

For the space discretization, we apply collocation based on quadratic splines. Let $\Delta^j \equiv \{x_0 \equiv \omega_a < x_1^j < x_2^j < \cdots < x_{N-1}^j < x_N \equiv \omega_b\}$ be the partition of Ω at time t_j and $U^j(x) = \sum_i c_i^j \phi_i^j(x)$ be the spline approximation to $u(x, t_j)$ written in terms of appropriate spline basis functions $\phi_i^j(x)$. Let also D^j be the set of collocation points at time t_j, where (4) is collocated. In the case of a uniform partition, we have $x_i^j = \omega_a + ih$, with $h = \frac{\omega_b - \omega_a}{N}$ for all j, and $D^j = \{\tau_i^j = (x_{i-1}^j + x_i^j)/2, i = 1, \ldots, N\}$. Let $u_I^j(x)$ be the quadratic-spline interpolant of u^j satisfying

$$u_I^j(x) = u^j(x), \;\; x = \omega_a, \;\; x \in D^j, \; x = \omega_b. \tag{5}$$

The standard spline collocation approximation $U^j(x)$, $j = 1, \ldots$, is computed by forcing it to satisfy (4) for $x \in D^j$, and the boundary conditions (2), that is, $\mathcal{B}^j U^j(x) = \gamma^j(x)$ at $x = \omega_a, \omega_b$. The initial approximation $U^0(x)$ is the quadratic-spline interpolant u_I^0 of u^0.

This spline collocation approximation turns out to be second-order, that is, non-optimal. In order to develop optimal spline collocation methods for Problem (1)-(3), we develop perturbations $\mathcal{P}_{\mathcal{L}}$ and $\mathcal{P}_{\mathcal{B}}$ of $\mathcal{L}$ and $\mathcal{B}$, respectively, similar to those used to obtain optimal spline collocation methods for BVPs; see for example [13]. Thus we have the *extrapolated* or *one-step* method (1QSC-CN) in which, with $u_\Delta^0 = u_I^0$, an optimal order approximation u_Δ^j is determined by the equations

$$\begin{aligned}(\mathcal{I} - \lambda h_t(\mathcal{L}^j + \mathcal{P}_{\mathcal{L}}^j))u_\Delta^j(x) &= (\mathcal{I} + (1-\lambda)h_t(\mathcal{L}^{j-1} + \mathcal{P}_{\mathcal{L}}^{j-1}))u_\Delta^{j-1}(x) + h_t(\lambda g^j(x) + (1-\lambda)g^{j-1}(x)), \; x \in D^j \\ (\mathcal{B}^j + \mathcal{P}_{\mathcal{B}}^j)u_\Delta^j(x) &= \gamma^j(x), \; x = \omega_a, \omega_b.\end{aligned} \tag{6}$$

We also have the *deferred-correction* or *two-step* method (2QSC-CN) that first computes a second-order approximation U^j by

$$\begin{aligned}(\mathcal{I} - \lambda h_t \mathcal{L}^j)U^j(x) &= (\mathcal{I} + (1-\lambda)h_t\mathcal{L}^{j-1})U^{j-1}(x) + h_t(\lambda g^j(x) + (1-\lambda)g^{j-1}(x)), \; x \in D^j, \\ \mathcal{B}^j U^j(x) &= \gamma^j(x), \; x = \omega_a, \omega_b.\end{aligned} \tag{7}$$

then an optimal order approximation u_Δ^j by

$$\begin{aligned}(\mathcal{I} - \lambda h_t \mathcal{L}^j)u_\Delta^j(x) &= (\mathcal{I} + (1-\lambda)h_t(\mathcal{L}^{j-1} + \mathcal{P}_{\mathcal{L}}^{j-1}))u_\Delta^{j-1}(x) + h_t\lambda\mathcal{P}_{\mathcal{L}}^j U^j(x) + h_t(\lambda g^j(x) + (1-\lambda)g^{j-1}(x)), x \in D^j, \\ \mathcal{B}^j u_\Delta^j(x) &= \gamma^j(x) - \mathcal{P}_{\mathcal{B}}^j U^j(x), \; x = \omega_a, \omega_b,\end{aligned} \tag{8}$$

with $U^0 = u_I^0$ and $u_\Delta^0 = u_I^0$. When $\lambda = 1/2$ the methods 1QSC-CN and 2QSC-CN give rise to discretization errors of $O(h_t^2 + h^4)$, locally at the gridpoints and midpoints of the space partition, where h is the (maximum) space partition stepsize.

Each set of equations (6), (7) and (8) results in a linear system to be solved. Method 1QSC-CN solves one (almost pentadiagonal) linear system per time step, while 2QSC-CN solves two but sparser (tridiagonal) linear systems. We propose yet another method that solves one linear system per time step with the same matrix as that arising from 2QSC-CN.

The method QSC-CN is an one-step, still non-extrapolated method, that computes u_Δ^j by the equations

$$\begin{aligned}(\mathcal{I} - \lambda h_t \mathcal{L}^j)u_\Delta^j(x) &= (\mathcal{I} + (1-\lambda)h_t\mathcal{L}^{j-1} + h_t\mathcal{P}_{\mathcal{L}}^{j-1}))u_\Delta^{j-1}(x) + h_t(\lambda g^j(x) + (1-\lambda)g^{j-1}(x)), \; x \in D^j, \\ \mathcal{B}^j u_\Delta^j(x) &= \gamma^j(x) - \mathcal{P}_{\mathcal{B}}^j u_\Delta^{j-1}(x), \; x = \omega_a, \omega_b,\end{aligned} \tag{9}$$

with $u^0_\Delta = u^0_I$. One can view this method as combining (7) and (8) into one equation and treating the term $h_t \lambda \mathcal{P}^j_{\mathcal{L}} U^j$ of (8) explicitly, i.e. substituting $\mathcal{P}^j_{\mathcal{L}} U^j$ by $\mathcal{P}^{j-1}_{\mathcal{L}} u^{j-1}_\Delta$.

The definitions of $\mathcal{P}_{\mathcal{L}}$ and $\mathcal{P}_{\mathcal{B}}$ are given in [13] for uniform grids, and in [6] for non-uniform grids. For the ease of the reader, we present here the definitions of $\mathcal{P}_{\mathcal{L}}$ and $\mathcal{P}_{\mathcal{B}}$ for uniform grids. Let $(\cdot)''$ and $(\cdot)'$ denote second and first derivatives, respectively, with respect to x. For any quadratic spline u_Δ with respect to Δ, we have

$$\mathcal{P}_{\mathcal{L}} u_\Delta(\tau_i) \equiv \frac{p(\tau_i)}{24}(u''_\Delta(\tau_{i-1}) - 2u''_\Delta(\tau_i) + u''_\Delta(\tau_{i+1})) - \frac{q(\tau_i)}{24}(u'_\Delta(\tau_{i-1}) - 2u'_\Delta(\tau_i) + u'_\Delta(\tau_{i+1})) \text{ at } \tau_i, i = 2, \ldots, N-1, \tag{10}$$

$$\mathcal{P}_{\mathcal{L}} u_\Delta(\tau_1) \equiv \frac{p(\tau_i)}{24}(2u''_\Delta(\tau_1) - 5u''_\Delta(\tau_2) + 4u''_\Delta(\tau_3) - u''_\Delta(\tau_4)) - \frac{q(\tau_i)}{24}(2u'_\Delta(\tau_1) - 5u'_\Delta(\tau_2) + 4u'_\Delta(\tau_3) - u'_\Delta(\tau_4)) \tag{11}$$

and similarly at $x = \tau_N$. We also have

$$\mathcal{P}_{\mathcal{B}} u_\Delta(x_0) \equiv \frac{\beta(x_0)}{24}(5u'_\Delta(\tau_1) - 13u'_\Delta(\tau_2) + 11u'_\Delta(\tau_3) - 3u'_\Delta(\tau_4)) \tag{12}$$

and similarly at $x = x_N$. We also present the matrices arising from (6) and (9) with $\lambda = 1/2$, and identify the terms corresponding to $\mathcal{P}_{\mathcal{L}}$ and $\mathcal{P}_{\mathcal{B}}$, in the case of uniform grids, and for certain boundary conditions. We remind readers that the space $\mathcal{M}$ of quadratic splines with respect to a partition Δ with N subintervals has dimension $N+2$, and a set of basis functions for $\mathcal{M}$ can be found in [4]. For the presentation of the constituent quadratic-spline collocation matrices, since we use uniform grids and the same grid partition at each time step, we drop the superscript j from the spatial points.

Both methods (6) and (9) give rise to linear systems of the form

$$A^j \vec{c}^j = B^{j-1} \vec{c}^{j-1} + \vec{g}^j, \tag{13}$$

where we have adopted the arrow $(\vec{\cdot})$ notation for vectors of length $N+2$. To give the forms of A^j and B^j, let $\xi \equiv \frac{h_t}{h^2}$, $D^j_p \equiv diag\{0, p^j(\tau_1), \ldots, p^j(\tau_N), 0\}$, $D^j_q \equiv diag\{0, q^j(\tau_1), \ldots, q^j(\tau_N), 0\}$, $D^j_r \equiv diag\{0, r^j(\tau_1), \ldots, r^j(\tau_N), 0\}$, $D^j_I \equiv diag\{0, 1, \ldots, 1, 0\}$, $D^j_\alpha \equiv diag\{\alpha^j(\omega_a), 0, \ldots, 0, \alpha^j(\omega_b)\}$, $D^j_\beta \equiv diag\{\beta^j(\omega_a), 0, \ldots, 0, \beta^j(\omega_b)\}$, where $diag\{\}$ denotes a diagonal matrix with the diagonal elements listed in the brackets. Let also

$$Q_0 = \frac{1}{8}\begin{bmatrix} 4 & 4 & 0 & 0 & \cdots & 0 \\ 1 & 6 & 1 & 0 & \cdots & 0 \\ \ddots & \ddots & \ddots & \ddots & \ddots & \ddots \\ 0 & \cdots & 0 & 1 & 6 & 1 \\ 0 & \cdots & 0 & 0 & 4 & 4 \end{bmatrix}, Q_1 = \frac{1}{2}\begin{bmatrix} -2 & 2 & 0 & 0\cdots & 0 \\ -1 & 0 & 1 & 0\cdots & 0 \\ \ddots & \ddots & \ddots & \ddots & \ddots \\ 0\cdots & 0 & -1 & 0 & 1 \\ 0\cdots & 0 & 0 & -2 & 2 \end{bmatrix}, Q_2 = \begin{bmatrix} 0 & 0 & 0 & 0\cdots & 0 \\ 1 & -2 & 1 & 0\cdots & 0 \\ \ddots & \ddots & \ddots & \ddots & \ddots \\ 0\cdots & 0 & 1 & -2 & 1 \\ 0\cdots & 0 & 0 & 0 & 0 \end{bmatrix}, \tag{14}$$

$$Q'_1 = \begin{bmatrix} 0 & -5 & 13 & -11 & 3 & 0\cdots & 0 \\ 0 & 2 & -5 & 4 & -1 & 0\cdots & 0 \\ 0 & 1 & -2 & 1 & 0 & 0\cdots & 0 \\ \ddots & \ddots & \ddots & \ddots & \ddots & \ddots & \ddots \\ 0\cdots & 0 & 0 & 1 & -2 & 1 & 0 \\ 0\cdots & 0 & -1 & 4 & -5 & 2 & 0 \\ 0\cdots & 0 & 3 & -11 & 13 & -5 & 0 \end{bmatrix}, Q'_2 = \begin{bmatrix} 0 & 0 & & & & \cdots & 0 \\ 0 & 2 & -5 & 4 & -1 & 0\cdots & 0 \\ 0 & 1 & -2 & 1 & 0 & 0\cdots & 0 \\ \ddots & \ddots & \ddots & \ddots & \ddots & \ddots & \ddots \\ 0\cdots & 0 & 0 & 1 & -2 & 1 & 0 \\ 0\cdots & 0 & -1 & 4 & -5 & 2 & 0 \\ 0\cdots & & & & & 0 & 0 \end{bmatrix}, \tag{15}$$

and

$$L^j = D^j_p Q_2 + h D^j_q Q_1 + h^2 D^j_r Q_0, \; P^j = \frac{1}{24} D^j_p Q'_2 Q_2 - \frac{h}{24} D^j_q Q'_1 Q_1. \tag{16}$$

For method (6),

$$A^j = D_I Q_0 - \frac{\xi}{2}(L^j + P^j) + D^j_\alpha Q_0 + \frac{1}{h} D^j_\beta Q_1 - \frac{1}{24h} D^j_\beta Q'_1 Q_1, \;\; B^j = D_I Q_0 + \frac{\xi}{2}(L^j + P^j). \tag{17}$$

In the above, L^j arises from the discretization of $\mathcal{L}$, P^j corresponds to $\mathcal{P}_{\mathcal{L}}$, and $D^j_\alpha Q_0 + \frac{1}{h} D^j_\beta Q_1 - \frac{1}{24h} D^j_\beta Q'_1 Q_1$ make up the terms related to $\mathcal{B}$ (first two terms) and $\mathcal{P}_{\mathcal{B}}$ (third term). For method (9),

$$A^j = D_I Q_0 - \frac{\xi}{2} L^j + D^j_\alpha Q_0 + \frac{1}{h} D^j_\beta Q_1, \quad B^j = D_I Q_0 + \frac{\xi}{2} L^j + \xi P^j + \frac{1}{24h} D^j_\beta Q'_1 Q_1. \tag{18}$$

For both methods (6) and (9),

$$\vec{g}^j = [\gamma^j(\omega_a), \frac{h_t}{2}(g^j(\tau_1) + g^{j-1}(\tau_1)), \ldots, \frac{h_t}{2}(g^j(\tau_N) + g^{j-1}(\tau_N)), \gamma^j(\omega_b)]^T. \tag{19}$$

Note that all matrices in (13)-(18) are of size $(N+2) \times (N+2)$.

For the purposes of the analysis, we consider two variants, $\hat{u}^j_I(x)$ and $\widehat{u^j_I}(x)$, of the interpolant u^j_I, and certain variants of the methods (6) and (9). These variants include an additional perturbation term on the boundary, on which we elaborate further in the paper. Let $\hat{u}^j_I(x)$ be the quadratic-spline interpolant of u^j satisfying

$$\hat{u}^j_I(x) = \begin{cases} u^j(x) - \dfrac{h^4}{128}(u^j)^{(4)}(x), & x = x_0,\ x = x_N \\ u^j(x), & x = \tau_i, 1 \le i \le N, \end{cases} \tag{20}$$

where $(u^j)^{(4)}$ denotes the fourth derivative with respect to x of u^j. Let $\widehat{u^j_I}$ be the quadratic-spline interpolant of u^j satisfying

$$\widehat{u^j_I}(x) = \begin{cases} u^j(x) - \dfrac{h^4}{128}\widehat{(u^j)^{(4)}}(x), & x = x_0,\ x = x_N \\ u^j(x), & x = \tau_i, 1 \le i \le N, \end{cases} \tag{21}$$

where $\widehat{(u^j)^{(4)}}$ is an approximation to $(u^j)^{(4)}$, which, for $j = 0$, is computed as described below. For any function $u \in \mathcal{C}^6[\Omega]$, i.e. a function u with bounded derivatives up to sixth order with respect to x in $\Omega \cup \partial\Omega$, it can be easily shown that

$$u^{(4)}(x_0) = \frac{640u(x_0) - 1512u(\tau_1) + 1848u(\tau_2) - 1512u(\tau_3) + 648u(\tau_4) - 112u(\tau_5)}{63h^4} + O(h^2). \tag{22}$$

Since $u^0(x)$ is given in Ω, an $O(h^2)$ approximation $\widehat{(u^0)^{(4)}}(x_0)$ to $(u^0)^{(4)}(x_0)$ can be computed by (22). A similar approximation can be computed at $x = x_N$. Thus, $\widehat{u^0_I}$ can be computed by (21) for $j = 0$. As will be shown later, $\widehat{u^0_I}$ is an $O(h^6)$ approximation to $\hat{u}^0_I$. We emphasize that $\hat{u}^j_I$, $j \ge 0$, is needed only for the analysis of the methods and not for the formulation, while $\widehat{u^0_I}$ is needed for the formulation as well as the analysis of the methods.
For any function $u \in \mathcal{C}^6[\Omega]$, it can also be shown that

$$u^{(4)}(x_0) = \frac{5u''(\tau_1) - 13u''(\tau_2) + 11u''(\tau_3) - 3u''(\tau_4)}{2h^2} + O(h^2). \tag{23}$$

We define $\mathcal{P}_I u^j_\Delta(x_0)$ by

$$\mathcal{P}_I u^j_\Delta(x_0) \equiv \frac{h^4}{128} \frac{5(u^j_\Delta)''(\tau_1) - 13(u^j_\Delta)''(\tau_2) + 11(u^j_\Delta)''(\tau_3) - 3(u^j_\Delta)''(\tau_4)}{2h^2}, \tag{24}$$

and $\mathcal{P}_I u^j_\Delta(x_N)$ by a similar relation. We consider the variant *1QSCB-CN* of method (6), in which, with $u^0_\Delta = \widehat{u^0_I}$, u^j_Δ is determined by the equations

$$\begin{aligned} (\mathcal{I} - \lambda h_t(\mathcal{L}^j + \mathcal{P}^j_{\mathcal{L}}))u^j_\Delta(x) &= (\mathcal{I} + (1-\lambda)h_t(\mathcal{L}^{j-1} + \mathcal{P}^{j-1}_{\mathcal{L}}))u^{j-1}_\Delta(x) + h_t(\lambda g^j(x) + (1-\lambda)g^{j-1}(x)),\ x \in D^j, \\ (\mathcal{B}^j + \mathcal{P}^j_{\mathcal{B}} + \mathcal{P}_I)u^j_\Delta(x) &= \gamma^j(x),\ x = \omega_a, \omega_b. \end{aligned} \tag{25}$$

and the variant *QSCB-CN* of method (9) in which, with $u_\Delta^0 = \widehat{u_I^0}$, u_Δ^j is determined by the equations

$$\begin{aligned}(\mathcal{I} - \lambda h_t \mathcal{L}^j) u_\Delta^j(x) &= (\mathcal{I} + (1-\lambda) h_t \mathcal{L}^{j-1} + h_t \mathcal{P}_{\mathcal{L}}^{j-1})) u_\Delta^{j-1}(x) + h_t(\lambda g^j(x) + (1-\lambda) g^{j-1}(x)),\ x \in D^j, \\ (\mathcal{B}^j + \mathcal{P}_I) u_\Delta^j(x) &= \gamma^j(x) - \mathcal{P}_{\mathcal{B}}^j u_\Delta^{j-1}(x),\ x = \omega_a, \omega_b.\end{aligned} \tag{26}$$

Clearly, we can also define a variant (2QSCB-CN) of method (7)-(8) in a similar way, however, we focus primarily on methods 1QSCB-CN and QSCB-CN.

3 Stability of 1QSCB-CN and 1QSC-CN

In this section, we consider the stability of 1QSCB-CN (method (25)) and 1QSC-CN (method (6)) for a model problem and uniform space partitions.

Consider the case $q = r = g = \beta = \gamma = 0$ and p constant, that is, the model problem

$$u_t - p u_{xx} = 0 \quad \text{in} \quad \Omega \times (0, T) \tag{27}$$

$$u = 0 \quad \text{on} \quad \partial\Omega \times (0, T) \tag{28}$$

$$u = u^0 \quad \text{on} \quad (\partial\Omega \cup \Omega) \times \{0\}. \tag{29}$$

For the PDE problem (27)-(29), using the quadratic-spline basis functions for $\mathcal{M}$ in [4], we write method (25) in a matrix form that is convenient for the analysis. Let $u_\Delta^j(x) = \sum_i c_i^j \phi_i(x)$ be the finite element representation of u_Δ^j. Using (24), we have

$$\mathcal{P}_I u_\Delta^j(x_0) = \frac{h^4}{128} \frac{5c_0^j - 23c_1^j + 42c_2^j - 38c_3^j + 17c_4^j - 3c_5^j}{2h^4}$$

thus the equation at $x = x_0$ is

$$\frac{1}{2}c_0^j + \frac{1}{2}c_1^j + \frac{h^4}{128} \frac{5c_0^j - 23c_1^j + 42c_2^j - 38c_3^j + 17c_4^j - 3c_5^j}{2h^4} = 0$$

from which we obtain

$$c_0^j = \frac{1}{133}(-105c_1^j - 42c_2^j + 38c_3^j - 17c_4^j + 3c_5^j). \tag{30}$$

Let $\sigma = p\xi$. The equation at $x = \tau_1$ is

$$\begin{aligned} & \tfrac{1}{8}c_0^j + \tfrac{3}{4}c_1^j + \tfrac{1}{8}c_2^j - \tfrac{\sigma}{2}(c_0^j - 2c_1^j + c_2^j) - \tfrac{\sigma}{48}(2c_0^j - 9c_1^j + 16c_2^j - 14c_3^j + 6c_4^j - c_5^j) \\ = \ & \tfrac{1}{8}c_0^{j-1} + \tfrac{3}{4}c_1^{j-1} + \tfrac{1}{8}c_2^{j-1} + \tfrac{\sigma}{2}(c_0^{j-1} - 2c_1^{j-1} + c_2^{j-1}) + \tfrac{\sigma}{48}(2c_0^{j-1} - 9c_1^{j-1} + 16c_2^{j-1} - 14c_3^{j-1} + 6c_4^{j-1} - c_5^{j-1}), \end{aligned}$$

which, after substitution of c_0^j and c_0^{j-1} using (30) accordingly, becomes

$$\begin{aligned} & \left(\left[\tfrac{99}{152}, \tfrac{13}{152}, \tfrac{1}{28}, \tfrac{-17}{1064}, \tfrac{3}{1064}\right] + \sigma\left[\tfrac{491}{304}, \tfrac{-151}{228}, \tfrac{23}{168}, \tfrac{-89}{1596}, \tfrac{55}{6384}\right]\right) \left[c_1^j, c_2^j, c_3^j, c_4^j, c_5^j\right]^T \\ = \ & \left(\left[\tfrac{99}{152}, \tfrac{13}{152}, \tfrac{1}{28}, \tfrac{-17}{1064}, \tfrac{3}{1064}\right] - \sigma\left[\tfrac{491}{304}, \tfrac{-151}{228}, \tfrac{23}{168}, \tfrac{-89}{1596}, \tfrac{55}{6384}\right]\right) \left[c_1^{j-1}, c_2^{j-1}, c_3^{j-1}, c_4^{j-1}, c_5^{j-1}\right]^T. \end{aligned} \tag{31}$$

The equation at $x = \tau_N$ can be derived in a similar way. The equation at $x = \tau_2$ is

$$\begin{aligned} & \tfrac{1}{8}c_1^j + \tfrac{3}{4}c_2^j + \tfrac{1}{8}c_3^j - \tfrac{\sigma}{2}(c_1^j - 2c_2^j + c_3^j) - \tfrac{\sigma}{48}(c_0^j - 4c_1^j + 6c_2^j - 4c_3^j + c_4^j) \\ = \ & \tfrac{1}{8}c_1^{j-1} + \tfrac{3}{4}c_2^{j-1} + \tfrac{1}{8}c_3^{j-1} + \tfrac{\sigma}{2}(c_1^{j-1} - 2c_2^{j-1} + c_3^{j-1}) - \tfrac{\sigma}{48}(c_0^{j-1} - 4c_1^{j-1} + 6c_2^{j-1} - 4c_3^{j-1} + c_4^{j-1}) \end{aligned}$$

which, after substitution of c_0^j and c_0^{j-1} using (30) accordingly, becomes

$$\begin{aligned} & \left(\left[\tfrac{1}{8}, \tfrac{3}{4}, \tfrac{1}{8}, 0, 0\right] + \sigma\left[\tfrac{-365}{912}, \tfrac{67}{76}, \tfrac{-71}{168}, \tfrac{-29}{1596}, \tfrac{-1}{2128}\right]\right) \left[c_1^j, c_2^j, c_3^j, c_4^j, c_5^j\right]^T \\ = \ & \left(\left[\tfrac{1}{8}, \tfrac{3}{4}, \tfrac{1}{8}, 0, 0\right] - \sigma\left[\tfrac{-365}{912}, \tfrac{67}{76}, \tfrac{-71}{168}, \tfrac{-29}{1596}, \tfrac{-1}{2128}\right]\right) \left[c_1^{j-1}, c_2^{j-1}, c_3^{j-1}, c_4^{j-1}, c_5^{j-1}\right]^T. \end{aligned} \tag{32}$$

The equation at $x = \tau_{N-1}$ can be derived in a similar way. The equation at $x = \tau_i, i = 3, \ldots, N-2$, is

$$\begin{aligned} & \left(\left[0, \tfrac{1}{8}, \tfrac{3}{4}, \tfrac{1}{8}, 0\right] + \sigma\left[\tfrac{-1}{48}, \tfrac{-5}{12}, \tfrac{7}{8}, \tfrac{-5}{12}, \tfrac{-1}{48}\right]\right)\left[c_{i-2}^j, c_{i-1}^j, c_i^j, c_{i+1}^j, c_{i+2}^j\right]^T \\ = \; & \left(\left[0, \tfrac{1}{8}, \tfrac{3}{4}, \tfrac{1}{8}, 0\right] - \sigma\left[\tfrac{-1}{48}, \tfrac{-5}{12}, \tfrac{7}{8}, \tfrac{-5}{12}, \tfrac{-1}{48}\right]\right)\left[c_{i-2}^{j-1}, c_{i-1}^{j-1}, c_i^{j-1}, c_{i+1}^{j-1}, c_{i+2}^{j-1}\right]^T. \end{aligned} \tag{33}$$

Thus, for the PDE problem (27)-(29), method (25) gives rise to linear systems of the form

$$A\vec{\vec{c}}^{\,j} = B\vec{\vec{c}}^{\,j-1}, \tag{34}$$

where we have dropped the superscript j from A and B, since p is constant, and we have adopted the double arrow $\vec{\vec{(\cdot)}}$ notation for vectors of length N, which arise as restrictions of vectors of length $N+2$ by omitting the first and last components. The matrices A and B of (25) for (27)-(29) take the form

$$A = A_0 + \sigma A_\sigma, \; B = A_0 - \sigma A_\sigma, \tag{35}$$

where

$$A_0 = \begin{bmatrix} \frac{99}{152} & \frac{13}{152} & \frac{1}{28} & \frac{-17}{1064} & \frac{3}{1064} & 0 & \cdots & 0 \\ \frac{1}{8} & \frac{3}{4} & \frac{1}{8} & 0 & 0 & 0 & \cdots & 0 \\ 0 & \frac{1}{8} & \frac{3}{4} & \frac{1}{8} & 0 & 0 & \cdots & 0 \\ \ddots & \ddots & \ddots & \ddots & \ddots & \ddots & \ddots & \ddots \\ 0 & \cdots & 0 & 0 & \frac{1}{8} & \frac{3}{4} & \frac{1}{8} & 0 \\ 0 & \cdots & 0 & 0 & 0 & \frac{1}{8} & \frac{3}{4} & \frac{1}{8} \\ 0 & \cdots & 0 & \frac{3}{1064} & \frac{-17}{1064} & \frac{1}{28} & \frac{13}{152} & \frac{99}{152} \end{bmatrix}, A_\sigma = \begin{bmatrix} \frac{491}{304} & \frac{-151}{228} & \frac{23}{168} & \frac{-89}{1596} & \frac{55}{6384} & 0 & \cdots & 0 \\ \frac{-365}{912} & \frac{67}{76} & \frac{-71}{168} & \frac{-29}{1596} & \frac{-1}{2128} & 0 & \cdots & 0 \\ \frac{-1}{48} & \frac{-5}{12} & \frac{7}{8} & \frac{-5}{12} & \frac{-1}{48} & 0 & \cdots & 0 \\ \ddots & \ddots & \ddots & \ddots & \ddots & \ddots & \ddots & \ddots \\ 0 & \cdots & 0 & \frac{-1}{48} & \frac{-5}{12} & \frac{7}{8} & \frac{-5}{12} & \frac{-1}{48} \\ 0 & \cdots & 0 & \frac{-1}{2128} & \frac{-29}{1596} & \frac{-71}{168} & \frac{67}{76} & \frac{-365}{912} \\ 0 & \cdots & 0 & \frac{55}{6384} & \frac{-89}{1596} & \frac{23}{168} & \frac{-151}{228} & \frac{491}{304} \end{bmatrix}, \tag{36}$$

For the 1QSC-CN method for the problem (27)-(29), we have, instead of (30), $c_0^j = -c_1^j$, and after some manipulation as above, we get linear systems of the form (34), with A and B as in (35), where

$$A_0 = \begin{bmatrix} \frac{5}{8} & \frac{1}{8} & 0 & 0 & 0 & 0 & \cdots & 0 \\ \frac{1}{8} & \frac{3}{4} & \frac{1}{8} & 0 & 0 & 0 & \cdots & 0 \\ 0 & \frac{1}{8} & \frac{3}{4} & \frac{1}{8} & 0 & 0 & \cdots & 0 \\ \ddots & \ddots & \ddots & \ddots & \ddots & \ddots & \ddots & \ddots \\ 0 & \cdots & 0 & 0 & \frac{1}{8} & \frac{3}{4} & \frac{1}{8} & 0 \\ 0 & \cdots & 0 & 0 & 0 & \frac{1}{8} & \frac{3}{4} & \frac{1}{8} \\ 0 & \cdots & 0 & 0 & 0 & 0 & \frac{1}{8} & \frac{5}{8} \end{bmatrix}, A_\sigma = \begin{bmatrix} \frac{83}{48} & \frac{-5}{6} & \frac{7}{24} & \frac{-1}{8} & \frac{1}{48} & 0 & \cdots & 0 \\ \frac{-19}{48} & \frac{7}{8} & \frac{-5}{12} & \frac{-1}{48} & 0 & 0 & \cdots & 0 \\ \frac{-1}{48} & \frac{-5}{12} & \frac{7}{8} & \frac{-5}{12} & \frac{-1}{48} & 0 & \cdots & 0 \\ \ddots & \ddots & \ddots & \ddots & \ddots & \ddots & \ddots & \ddots \\ 0 & \cdots & 0 & \frac{-1}{48} & \frac{-5}{12} & \frac{7}{8} & \frac{-5}{12} & \frac{-1}{48} \\ 0 & \cdots & 0 & 0 & \frac{-1}{48} & \frac{-5}{12} & \frac{7}{8} & \frac{-19}{48} \\ 0 & \cdots & 0 & \frac{1}{48} & \frac{-1}{8} & \frac{7}{24} & \frac{-5}{6} & \frac{83}{48} \end{bmatrix}, \tag{37}$$

Note that all matrices in (34)-(37) are of size $N \times N$.

According to [16], a method is stable if the numerical solutions at all timesteps are bounded independently of h. While [16] uses the scaled Euclidean norm $||\vec{\vec{c}}^{\,j}||_2 \equiv (\sum(\vec{\vec{c}}_i^{\,j})^2/N)^{1/2}$ to study the boundedness of the numerical solutions, we will use the uniform (maximum) norm $||\vec{\vec{c}}^{\,j}||_\infty \equiv \max\{|\vec{\vec{c}}_i^{\,j}|\}$, since $||\vec{\vec{c}}^{\,j}||_2 \leq ||\vec{\vec{c}}^{\,j}||_\infty$. For methods described by (34), with $Q = A^{-1}B$ being the "iteration" matrix and Q^j the jth power of Q, if $\lim_{h\to 0}(\max_{j=0,1,\ldots,T/h_t} ||Q^j||_\infty)$ is bounded independently of h, the stability of the method is ensured.

To study the stability properties of 1QSCB-CN, for the problem (27)-(29), we consider $Q = A^{-1}B$, with A and B as in (35), and A_0 and A_σ as in (36), and show numerically the boundedness of $||Q^j||_\infty$ as h and h_t tend to 0. We considered the quantities $||Q^j||_\infty$, with $h = 1/N$ and $h_t = \sigma h^2$, for several values of σ and N. Figures 1 and 2 show how $||Q^j||_\infty$ behaves as j increases, for several values of N, with $\sigma = 20$ (i.e. $h_t = 20h^2$), for the 1QSCB-CN and 1QSC-CN methods, respectively. Although $||Q^j||_\infty$ does not necessarily converge monotonically to 0, we can

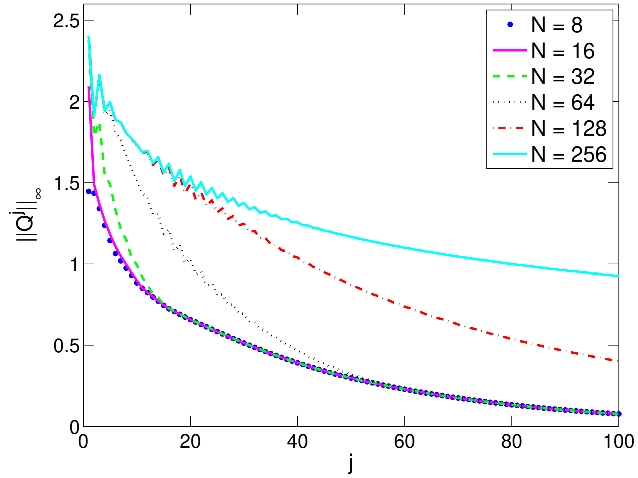

Figure 1: The powers of the iteration matrix for the 1QSCB-CN method applied to problem (27)-(29);σ=20.

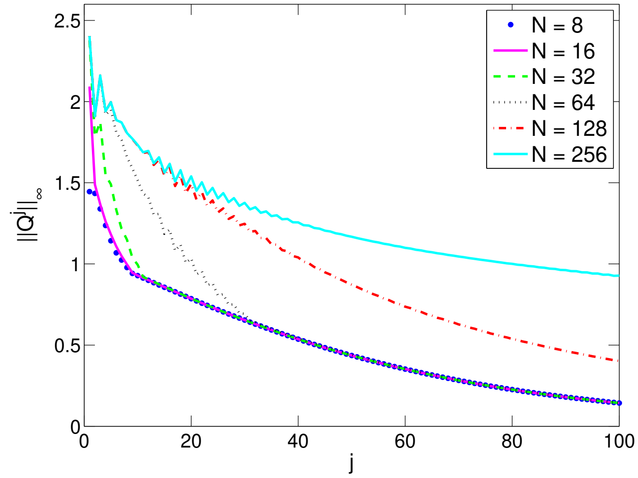

Figure 2: The powers of the iteration matrix for the 1QSC-CN method applied to problem (27)-(29); σ =20.

safely claim that $||Q^j||_\infty \leq ||Q||_\infty \leq \kappa$, where κ is independent of N, and thus $\lim_{h\to 0}(\max_{j=0,1,\ldots,T/h_t} ||Q^j||_\infty)$ is bounded independently of h. Thus, the 1QSCB-CN and 1QSC-CN methods for the PDE problem (27)-(29) are stable without restriction for the time stepsize.

Remark 1 In Table 1, we show the quantity $||Q^m||_\infty$, for $m = T/h_t$, with $T = 1$, for several values of N and σ, for the 1QSCB-CN and 1QSC-CN methods. The results indicate that this quantity, which can be viewed as the "amplification" factor of the error at the last time step, is bounded as $h = 1/N$ and $h_t = \sigma h^2$ tend to 0.

Table 1: The quantity $||Q^m||_\infty$, $m = T/h_t$, for methods 1QSCB-CN and 1QSC-CN applied to problem (27)-(29).

σ	$N = 8$	$N = 16$	$N = 32$	$N = 64$	$N = 128$	$N = 256$
			1QSCB-CN			
2	0.000167	0.000065	0.000066	0.000066	0.000066	0.000066
5	0.282730	0.003941	0.000065	0.000065	0.000066	0.000066
20	1.238369	0.798287	0.282896	0.004304	0.000065	0.000066
40	1.410485	1.300215	0.798100	0.286617	0.004304	0.000066
80	1.173207	1.644080	1.332475	0.798054	0.288491	0.004304
			1QSC-CN			
2	0.000718	0.000065	0.000066	0.000066	0.000066	0.000066
5	0.418006	0.011125	0.000065	0.000065	0.000066	0.000066
20	1.237141	0.885977	0.418091	0.011997	0.000065	0.000066
40	1.409175	1.300139	0.885877	0.422545	0.011999	0.000066
80	1.172702	1.644068	1.332474	0.885852	0.424785	0.011999

Remark 2 In Figure 3, we plot the spectral radii of the 1QSCB-CN iteration matrix versus σ for different values of N. Based on Figure 3, we can make some interesting comments, besides the fact that the spectral radii are less than one for all σ, a fact that is expected given the stability properties of 1QSCB-CN discussed above. For a fixed N, there is an optimal σ, which minimizes the spectral radii, for instance, the optimal σ for $N = 8$ is about 2. In addition, this optimal σ seems to be proportional to $\ln N$. For a fixed σ, the spectral radii become larger as N increases. But as σ increases, the spectral radii behave almost in the same way no matter what N is. Furthermore,

the larger N is, the less sensitive the spectral radii are to the values of σ. We may expect that the spectral radii tend to one as N tends to infinity for all σ. The spectral radii of the 1QSC-CN method, plotted in Figure 4, behave almost identically to those of 1QSCB-CN. It is worth mentioning that the spectral radii of the 1QSC-CN method for $N = 128, 256$ are the same as those of 1QSCB-CN, within six-digits precision.

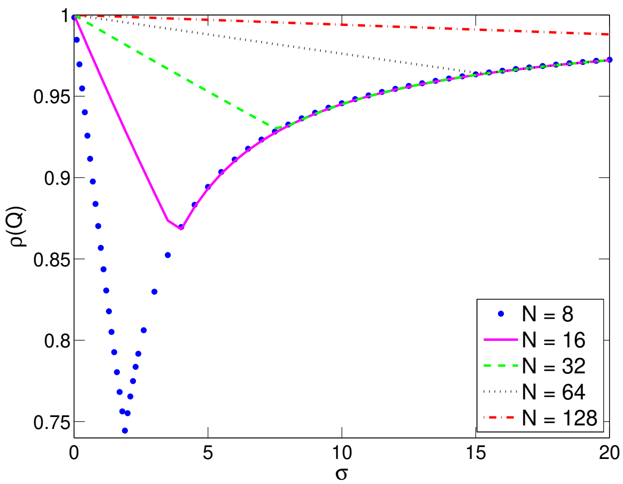

Figure 3: The spectral radii of the iteration matrix for the 1QSCB-CN method applied to problem (27)-(29).

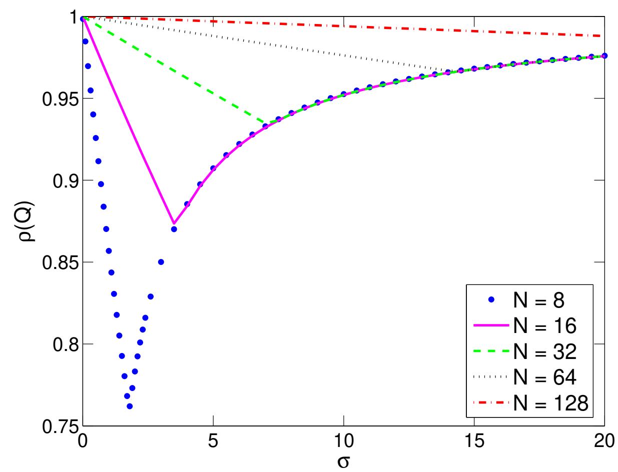

Figure 4: The spectral radii of the iteration matrix for the 1QSC-CN method applied to problem (27)-(29).

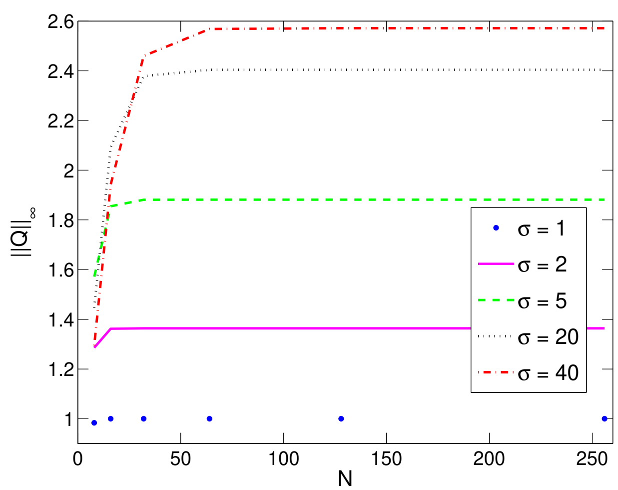

Figure 5: The infinity norm of the iteration matrix for the 1QSCB-CN method applied to problem (27)-(29).

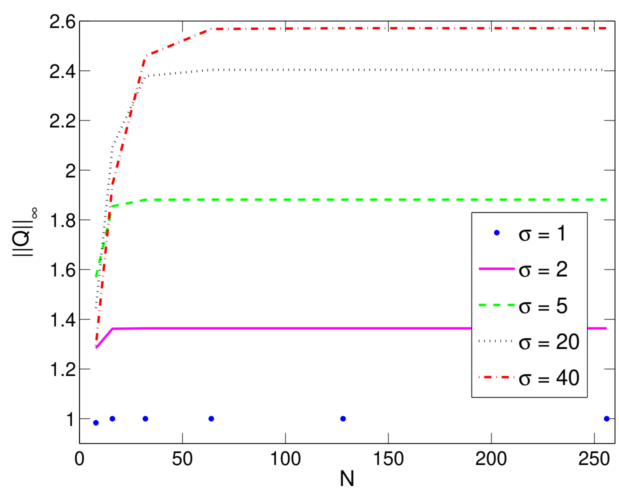

Figure 6: The infinity norm of the iteration matrix for the 1QSC-CN method applied to problem (27)-(29).

Remark 3 Given Lemma 1 in the next section, and the form of B in (35) with A_0 and A_σ as in (36), it is easy to prove that the norm $||Q||_\infty$ of matrix $Q = A^{-1}B$ of the 1QSCB-CN method is bounded independently of h. To visualize the boundedness of $||Q||_\infty$, in Figure 5, we plot $||Q||_\infty$ versus N for several values of σ. In a similar way as in Lemma 1, we can show that the inverse of matrix A in (35) with A_0 and A_σ as in (37) exists, and $||A^{-1}||_\infty$ is bounded independently of h, and that the norm $||Q||_\infty$ of matrix $Q = A^{-1}B$ with A and B as in (35), and A_0 and A_σ as in (37) (i.e. Q of the 1QSC-CN method) is bounded independently of h; see also Figure 6.

4 Convergence of 1QSCB-CN

In this section, we study the convergence of the 1QSCB-CN method with $\lambda = \frac{1}{2}$ for the PDE problem (27)-(29). We assume uniform space and time partitions with h and h_t the respective stepsizes, therefore the superscript denoting timestep index is dropped from the notation of the partition and collocation points. Let $M = \frac{T}{h_t}$ be the number of time steps. (If $\frac{T}{h_t}$ is not an integer, the time stepsize of the last time step is adjusted accordingly.)

Initially, according to the 1QSCB-CN method, $u^0_\Delta = \widehat{u^0_I}$. We assume that the initial solution function $u^0(x) \in \mathcal{C}^6[\Omega]$, and since, for a parabolic problem the solution at later time steps cannot be less smooth than the initial solution, we also have $u(x,t) \in \mathcal{C}^6[\Omega]$ (with respect to x) for all $t \in [0,T]$. Since $u(x,t)$ satisfies (27), we also have that u_{ttt} and u_{xxtt} are bounded for all x and t.

Discretizing the time variable in (27) with the Crank-Nicolson Method, and using Taylor's expansions, we get

$$u^j - \frac{1}{2}h_t\mathcal{L}u^j = u^{j-1} + \frac{1}{2}h_t\mathcal{L}u^{j-1} + h_t R^j, \tag{38}$$

where

$$R^j \equiv \frac{h_t^2}{24}u_{ttt}^{j_1} - \frac{h_t^2}{16}(u_{xxtt}^{j_2} + u_{xxtt}^{j_3}),\ j_1 \in [j-1,j],\ j_2 \in [j-1, j-\frac{1}{2}],\ j_3 \in [j-\frac{1}{2}, j]. \tag{39}$$

Clearly,

$$R^j = O(h_t^2),\ \text{for all } x,\ t \text{ and } j > 0. \tag{40}$$

We next summarize, in Theorem 1, some results directly derived from [13].

THEOREM 1 *According to [13], under the assumption $u^0 \in \mathcal{C}^6[\Omega]$, we have, for $j = 0, \ldots, M$,*

$$\begin{aligned}
\|(\hat{u}_I^j)^{(k)} - (u^j)^{(k)}\|_\infty &= O(h^{3-k}),\ k = 0,1,2 \\
\hat{u}_I^j(x) - u^j(x) &= O(h^4),\ \textit{for } x = x_i \\
(\hat{u}_I^j)'(x) - (u^j)'(x) &= O(h^3),\ \textit{for } x = x_i + \lambda h,\ \lambda = (3 \pm \sqrt{3})/6 \\
(\hat{u}_I^j)''(x) - (u^j)''(x) &= -\frac{h^2}{24}(u^j)^{(4)}(x) + O(h^2),\ \textit{for } x = \tau_i \qquad (41) \\
\hat{u}_I^j(x) - u^j(x) &= 0,\ \textit{for } x = \tau_i, \qquad (42) \\
(\mathcal{L} + \mathcal{P}_\mathcal{L})\hat{u}_I^j(x) - \mathcal{L}u^j(x) &= O(h^4),\ \textit{for } x = \tau_i. \qquad (43)
\end{aligned}$$

Taking into account relation (41) of Theorem 1, relation (23) and the definitions of $\mathcal{P}_I$ in (24), and of $\hat{u}_I^j$ in (20), it follows that

$$\mathcal{P}_I\hat{u}^j(x) = \frac{h^4}{128}(u^j)^{(4)}(x) + O(h^6),\ \text{for } x = x_0,\ x = x_N, \tag{44}$$

from which we also get

$$\hat{u}_I^j(x) - u^j(x) = -\mathcal{P}_I\hat{u}^j(x) + O(h^6),\ \text{for } x = x_0,\ x = x_N. \tag{45}$$

Let $\hat{u}_I^j(x) = \sum_{i=0}^{N+1} \hat{c}_i^j \phi_i^j(x)$ and $\widehat{u_I^j}(x) = \sum_{i=0}^{N+1} \widehat{c}_i^j \phi_i^j(x)$ be the finite element representation of $\hat{u}_I^j$ and $\widehat{u_I^j}$ defined by (20) and (21), respectively. Since the inverse of the quadratic-spline interpolation matrix is bounded in the uniform norm independently of h, we have $||\vec{\widehat{c^j}} - \vec{\hat{c}^j}||_\infty = O(h^6)$.

LEMMA 1 *The inverse of matrix A in (35) with A_0 and A_σ as in (36) exists, and $||A^{-1}||_\infty$ is bounded independently of h.*

Proof: Writing down the matrix A explicitly, by simple mathematical manipulation, we have, for $i = 1, \ldots, N$,

$$|A_{ii}| \geq \sum_{j=1, j\neq i}^{N} |A_{ij}| + \frac{1}{2}.$$

This leads to the desired result. □

For later convenience, let

$$R_1^j \equiv \mathcal{L}u^j - (\mathcal{L} + \mathcal{P}_\mathcal{L})\hat{u}_I^j, \tag{46}$$

and notice that from (43) we have

$$R_1^j = O(h^4), \text{ for } x = \tau_i \text{ and } j \geq 0. \tag{47}$$

We now come to the main convergence theorem.

THEOREM 2 *If $u^0 \in \mathcal{C}^6[\Omega]$ and $h_t = O(h^2)$, we have for $j = 0, \ldots, M$,*

$$\begin{aligned}
\|(u_\Delta^j)^{(k)} - (u^j)^{(k)}\|_\infty &= O(h^{3-k}),\ k = 0, 1, 2\\
|u_\Delta^j(x) - u^j(x)| &= O(h^4),\ \textit{for } x = x_i \textit{ and } x = \tau_i\\
|(u_\Delta^j)'(x) - (u^j)'(x)| &= O(h^3),\ \textit{for } x = x_i + \lambda h,\ \lambda = (3 \pm \sqrt{3})/6\\
|(u_\Delta^j)''(x) - (u^j)''(x)| &= O(h^2),\ \textit{for } x = \tau_i.
\end{aligned}$$

Proof: We first prove that at each time step t_j

$$\|(u_\Delta^j)^{(k)} - (\hat{u}_I^j)^{(k)}\|_\infty = t_j O(h^{4-k}),\ k = 0, 1, 2. \tag{48}$$

All the following equations are satisfied at the collocation points τ_i, $i = 1, \ldots, N$, unless otherwise indicated. We ignore terms with order higher than $O(h^4)$.

By relations (42) and (43) in Theorem 1, and by the definition of R_1^j in (46), we have

$$\hat{u}_I^j - \frac{1}{2}h_t(\mathcal{L} + \mathcal{P}_\mathcal{L})\hat{u}_I^j = u^j - \frac{1}{2}h_t\mathcal{L}u^j + \frac{1}{2}h_t R_1^j. \tag{49}$$

Using (38), relation (49) is rewritten as

$$\hat{u}_I^j - \frac{1}{2}h_t(\mathcal{L} + \mathcal{P}_\mathcal{L})\hat{u}_I^j = u^{j-1} + \frac{1}{2}h_t\mathcal{L}u^{j-1} + h_t(R^j + \frac{1}{2}R_1^j). \tag{50}$$

Using (42), (43) and (46) again, relation (50) becomes

$$\hat{u}_I^j - \frac{1}{2}h_t(\mathcal{L} + \mathcal{P}_\mathcal{L})\hat{u}_I^j = \hat{u}_I^{j-1} + \frac{1}{2}h_t(\mathcal{L} + \mathcal{P}_\mathcal{L})\hat{u}_I^{j-1} + h_t(R^j + \frac{1}{2}R_1^j + \frac{1}{2}R_1^{j-1}). \tag{51}$$

Define

$$\epsilon^j \equiv R^j + \frac{1}{2}R_1^j + \frac{1}{2}R_1^{j-1}, \tag{52}$$

and notice that, from (40) and (47), we have

$$\epsilon^j = O(h_t^2 + h^4), \tag{53}$$

which, by letting $h_t = O(h^2)$, gives

$$\epsilon^j = O(h^4). \tag{54}$$

By (45), we have

$$\hat{u}_I^j + \mathcal{P}_I\hat{u}_I^j = \gamma^j + O(h^6) \quad \text{at } x = x_0, x = x_N. \tag{55}$$

Relations (51), taking into account (55), after some manipulation, lead to the matrix equations

$$A\vec{\hat{c}}_I^{\,j} = B\vec{\hat{c}}_I^{\,j-1} + h_t\vec{\epsilon}^{\,j} + \vec{\zeta}^{\,j}, \tag{56}$$

where A and B are given in (35), and $\vec{\zeta}^{\,j}$ is a vector with $\zeta_i^j = 0$, for $i = 2, \ldots, N-1$, and $\zeta_i^j = O(h^6)$, for $i = 1, N$, i.e.

$$\|\vec{\zeta}^{\,j}\|_\infty = O(h^6). \tag{57}$$

Note that the non-zero components of $\vec{\zeta}^{\,j}$ arise from the $O(h^6)$ term in (55), after appropriate manipulation. Thus

$$\vec{\hat{c}}_I^{\,j} = A^{-1}B\vec{\hat{c}}_I^{\,j-1} + A^{-1}h_t\vec{\epsilon}^{\,j} + A^{-1}\vec{\zeta}^{\,j}. \tag{58}$$

We define

$$\vec{\varepsilon}^{\,j} \equiv A^{-1}\vec{\epsilon}^{\,j} + A^{-1}\vec{\zeta}^{\,j}/h_t. \tag{59}$$

By Lemma 1, and relations (54) and (57), we have

$$\|\vec{\varepsilon}^{\,j}\|_\infty = O(h^4). \tag{60}$$

Rewrite (58) as

$$\vec{\hat{c}}_I^{\,j} = A^{-1}B\vec{\hat{c}}_I^{\,j-1} + h_t\vec{\varepsilon}^{\,j}. \tag{61}$$

According to the 1QSCB-CN method, we have

$$\vec{c}^{\,j} = A^{-1}B\vec{c}^{\,j-1}. \tag{62}$$

Subtracting (62) from (61), we have

$$\vec{\hat{c}}_I^{\,j} - \vec{c}^{\,j} = Q(\vec{\hat{c}}_I^{\,j-1} - \vec{c}^{\,j-1}) + h_t\vec{\varepsilon}^{\,j}, \tag{63}$$

where we recall that $Q = A^{-1}B$ is the iteration matrix of the 1QSCB-CN method. It can be easily shown by induction that

$$\vec{\hat{c}}_I^{\,j} - \vec{c}^{\,j} = Q^j(\vec{\hat{c}}_I^{\,0} - \vec{c}^{\,0}) + h_t(Q^{j-1}\vec{\varepsilon}^{\,1} + Q^{j-2}\vec{\varepsilon}^{\,2} + \ldots + Q\vec{\varepsilon}^{\,j-1} + \vec{\varepsilon}^{\,j}). \tag{64}$$

Since $||Q^j||_\infty$ is bounded (see Section 3), we have for $m = 0, \ldots, j-1$

$$\|Q^m\vec{\varepsilon}^{\,j-m}\|_\infty = O(h^4).$$

Moreover, since $\vec{c}^{\,0} = \vec{\hat{c}}_I^{\,0} = \vec{c}_I^{\,0} + O(h^6)$, we have $||Q^j(\vec{\hat{c}}_I^{\,0} - \vec{c}^{\,0})||_\infty = O(h^6)$. Then, from (64), we get

$$\|\vec{\hat{c}}_I^{\,j} - \vec{c}^{\,j}\|_\infty = t_jO(h^4). \tag{65}$$

By noting that $c_0^j = \frac{1}{133}(-105c_1^j - 42c_2^j + 38c_3^j - 17c_4^j + 3c_5^j)$ and $\hat{c}_0^j = \frac{1}{133}(-105\hat{c}_1^j - 42\hat{c}_2^j + 38\hat{c}_3^j - 17\hat{c}_4^j + 3\hat{c}_5^j) + O(h^6)$, and the respective relations for c_{N+1}^j and $\hat{c}_{N+1}^j$, we get

$$\|\vec{\hat{c}}_I^{\,j} - \vec{c}^{\,j}\|_\infty = t_jO(h^4),$$

Noting that the quadratic-spline basis functions are bounded, we obtain (48). Finally, by Theorem 1 and the use of the triangle inequality, the desired results are easily obtained. $\square$

Here we make a remark regarding the convergence of 1QSC-CN. The technique for proving the convergence orders of 1QSCB-CN used in Theorem 2 cannot be directly applied to study the convergence of 1QSC-CN. The primary reason is that the approximation u_Δ of 1QSC-CN satisfies $u_\Delta^j = \gamma^j$ and not $u_\Delta^j + \mathcal{P}_I u_\Delta^j = \gamma^j$ on the boundary, and, therefore, the boundary equations of 1QSC-CN do not match the respective interpolant equations (55), and thus 1QSC-CN does not lead to the matrix equations (62). Furthermore, we note that the quadratic-spline interpolant u_I^j defined in (5) does not satisfy (41) and (43). The analysis of the convergence of 1QSC-CN remains an open problem. However, as shown in Section 7, all numerical results indicate that the approximation computed by 1QSC-CN satisfies the same error bounds as the one computed by 1QSCB-CN, that is, the perturbation $\mathcal{P}_I$ for the boundary equations is needed only for the analysis of the method.

Moreover, we remark that if we had not made the assumption $u^0 \in \mathcal{C}^6[\Omega]$ (and therefore $u \in \mathcal{C}^6[\Omega]$), we would not have been able to use the results from [13], summarized in Theorem 1. However, as in [13], numerical results given in Section 7 indicate that this assumption is only a sufficient and not necessary condition for convergence.

5 Properties of QSCB-CN, QSC-CN and improvements

From the description of the matrices corresponding to 1QSCB-CN and 1QSC-CN, it is clear that, at each time step, the main computational requirement of these methods is the solution of one pentadiagonal linear system. In this section, we focus on methods that, at each time step, require the solution of one tridiagonal linear system, namely methods QSCB-CN, QSC-CN and some new methods which we introduce.

We first study the stability of QSCB-CN (method (26)) and QSC-CN (method (9)) for the model problem (27)-(29) and uniform space partitions. Both methods QSCB-CN and QSC-CN result, after some manipulation, in linear systems of the form (34), with

$$A = A_0 + \sigma A_\sigma, \; B = A_0 - \sigma B_\sigma, \tag{66}$$

where A_0 is given in (36) for QSCB-CN, and in (37) for QSC-CN, while

$$A_\sigma = \begin{bmatrix} \frac{53}{38} & \frac{-13}{38} & \frac{-1}{7} & \frac{17}{266} & \frac{-3}{266} & 0 & \cdots & 0 \\ \frac{-1}{2} & 1 & \frac{-1}{2} & 0 & 0 & 0 & \cdots & 0 \\ 0 & \frac{-1}{2} & 1 & \frac{-1}{2} & 0 & 0 & \cdots & 0 \\ \ddots & \ddots & \ddots & \ddots & \ddots & \ddots & \ddots & \ddots \\ 0 & \cdots & 0 & 0 & \frac{-1}{2} & 1 & \frac{-1}{2} & 0 \\ 0 & \cdots & 0 & 0 & 0 & \frac{-1}{2} & 1 & \frac{-1}{2} \\ 0 & \cdots & 0 & \frac{-3}{266} & \frac{17}{266} & \frac{-1}{7} & \frac{-13}{38} & \frac{53}{38} \end{bmatrix}, B_\sigma = \begin{bmatrix} \frac{279}{152} & \frac{-56}{57} & \frac{5}{12} & \frac{-10}{57} & \frac{13}{456} & 0 & \cdots & 0 \\ \frac{-137}{456} & \frac{29}{38} & \frac{-29}{84} & \frac{-29}{798} & \frac{-1}{1064} & 0 & \cdots & 0 \\ \frac{-1}{24} & \frac{-1}{3} & \frac{3}{4} & \frac{-1}{3} & \frac{-1}{24} & 0 & \cdots & 0 \\ \ddots & \ddots & \ddots & \ddots & \ddots & \ddots & \ddots & \ddots \\ 0 & \cdots & 0 & \frac{-1}{24} & \frac{-1}{3} & \frac{3}{4} & \frac{-1}{3} & \frac{-1}{24} \\ 0 & \cdots & 0 & \frac{-1}{1064} & \frac{-29}{798} & \frac{-29}{84} & \frac{29}{38} & \frac{-137}{456} \\ 0 & \cdots & 0 & \frac{13}{456} & \frac{-10}{57} & \frac{5}{12} & \frac{-56}{57} & \frac{279}{152} \end{bmatrix}, \tag{67}$$

for QSCB-CN, and

$$A_\sigma = \begin{bmatrix} \frac{3}{2} & \frac{-1}{2} & 0 & 0 & 0 & 0 & \cdots & 0 \\ \frac{-1}{2} & 1 & \frac{-1}{2} & 0 & 0 & 0 & \cdots & 0 \\ 0 & \frac{-1}{2} & 1 & \frac{-1}{2} & 0 & 0 & \cdots & 0 \\ \ddots & \ddots & \ddots & \ddots & \ddots & \ddots & \ddots & \ddots \\ 0 & \cdots & 0 & 0 & \frac{-1}{2} & 1 & \frac{-1}{2} & 0 \\ 0 & \cdots & 0 & 0 & 0 & \frac{-1}{2} & 1 & \frac{-1}{2} \\ 0 & \cdots & 0 & 0 & 0 & 0 & \frac{-1}{2} & \frac{3}{2} \end{bmatrix}, B_\sigma = \begin{bmatrix} \frac{47}{24} & \frac{-7}{6} & \frac{7}{12} & \frac{-1}{4} & \frac{1}{24} & 0 & \cdots & 0 \\ \frac{-7}{24} & \frac{3}{4} & \frac{-1}{3} & \frac{-1}{24} & 0 & 0 & \cdots & 0 \\ \frac{-1}{24} & \frac{-1}{3} & \frac{3}{4} & \frac{-1}{3} & \frac{-1}{24} & 0 & \cdots & 0 \\ \ddots & \ddots & \ddots & \ddots & \ddots & \ddots & \ddots & \ddots \\ 0 & \cdots & 0 & \frac{-1}{24} & \frac{-1}{3} & \frac{3}{4} & \frac{-1}{3} & \frac{-1}{24} \\ 0 & \cdots & 0 & 0 & \frac{-1}{24} & \frac{-1}{3} & \frac{3}{4} & \frac{-7}{24} \\ 0 & \cdots & 0 & \frac{1}{24} & \frac{-1}{4} & \frac{7}{12} & \frac{-7}{6} & \frac{47}{24} \end{bmatrix}, \tag{68}$$

for QSC-CN.

Table 2: The spectral radii of the iteration matrix for the QSCB-CN method applied to problem (27)-(29).

σ	$N=8$	$N=16$	$N=32$	$N=64$	$N=128$	$N=256$
0.01	0.998459	0.999615	0.999904	0.999976	0.999994	0.999998
0.10	0.984698	0.996152	0.999037	0.999759	0.999940	0.999985
0.25	0.962182	0.990408	0.997593	0.999398	0.999849	0.999962
0.50	0.925776	0.980908	0.995192	0.998796	0.999699	0.999925
1.00	0.856896	0.962177	0.990408	0.997593	0.999398	0.999849
1.50	0.792805	0.943798	0.985646	0.996392	0.999097	0.999774
2.00	0.855119	0.925761	0.980908	0.995192	0.998796	0.999699
2.50	0.900826	0.908055	0.976191	0.993994	0.998495	0.999624
3.00	0.931590	0.931326	0.971497	0.992797	0.998194	0.999548
4.00	0.969668	0.969579	0.969579	0.990408	0.997593	0.999398
5.00	0.991968	0.991848	0.991848	0.991848	0.996993	0.999247
5.25	0.996144	0.995974	0.995974	0.995974	0.996842	0.999210
5.48	0.999613	0.999399	0.999399	0.999399	0.999399	0.999399
5.49	0.999756	0.999540	0.999540	0.999540	0.999540	0.999540
5.50	0.999899	0.999681	0.999681	0.999681	0.999681	0.999681
5.51	1.000041	0.999821	0.999821	0.999821	0.999821	0.999821
5.53	1.000324	1.000100	1.000100	1.000100	1.000100	1.000100
6.00	1.006359	1.006050	1.006050	1.006050	1.006050	1.006050

Table 3: The spectral radii of the iteration matrix for the QSC-CN method applied to problem (27)-(29).

σ	$N=8$	$N=16$	$N=32$	$N=64$	$N=128$	$N=256$
0.01	0.998459	0.999615	0.999904	0.999976	0.999994	0.999998
0.10	0.984698	0.996152	0.999037	0.999759	0.999940	0.999985
0.25	0.962183	0.990408	0.997593	0.999398	0.999849	0.999962
0.50	0.925778	0.980908	0.995192	0.998796	0.999699	0.999925
1.00	0.856901	0.962177	0.990408	0.997593	0.999398	0.999849
1.50	0.808801	0.943798	0.985646	0.996392	0.999097	0.999774
2.00	0.875518	0.925761	0.980908	0.995192	0.998796	0.999699
2.50	0.916844	0.916546	0.976191	0.993994	0.998495	0.999624
3.00	0.944600	0.944349	0.971497	0.992797	0.998194	0.999548
4.00	0.978890	0.978823	0.978823	0.990408	0.997593	0.999398
5.00	0.998995	0.998853	0.998853	0.998853	0.998853	0.999247
5.02	0.999310	0.999165	0.999165	0.999165	0.999165	0.999244
5.04	0.999623	0.999474	0.999474	0.999474	0.999474	0.999474
5.05	0.999779	0.999627	0.999627	0.999627	0.999627	0.999627
5.06	0.999934	0.999780	0.999780	0.999780	0.999780	0.999780
5.07	1.000088	0.999932	0.999932	0.999932	0.999932	0.999932
5.08	1.000241	1.000083	1.000083	1.000083	1.000083	1.000083
6.00	1.011928	1.011599	1.011599	1.011599	1.011599	1.011599

To study the stability properties of QSCB-CN and 1QSC-CN, for the problem (27)-(29), we follow a similar approach as for 1QSCB-CN and 1QSC-CN. However, for these methods, there are cases where the spectral radius of the iteration matrix is greater than one, therefore, there are restrictions on the stepsize to preserve stability. More specifically, we first study numerically the spectral radii of QSCB-CN, i.e. of $Q = A^{-1}B$, with A and B as in (66), A_0 as in (36), A_σ and B_σ as in (67). Table 2 shows selected results. The respective spectral radii for the QSC-CN method are shown in Table 3. In Figures 7 and 8, we plot the spectral radii of QSCB-CN and QSC-CN, respectively, versus σ for different values of N. From Table 2 and Figure 7, we see that, for QSCB-CN, $\rho(Q) < 1$, if $\sigma \leq 5.5$. For the QSC-CN method, we have $\rho(Q) < 1$, if $\sigma \leq 5.06$. Figures 9 and 10 show how $||Q^j||_\infty$ behaves as j increases, for several values of N, with $\sigma = 5.5$ for QSCB-CN and $\sigma = 5.06$ for QSC-CN, respectively. It is worth noting that the quantity $||Q^j||_\infty$ is rather insensitive to N for both methods. From the results, we have that, if $\sigma \leq 5.5$ for QSCB-CN, and if $\sigma \leq 5.06$ for QSC-CN, $\lim_{h\to 0}(\max_{j=0,1,\ldots,T/h_t} ||Q^j||_\infty)$ is bounded independently of h, thus the stability of the QSCB-CN and QSC-CN methods for the PDE problem (27)-(29) is obtained, under the condition $\sigma \leq 5.5$ and $\sigma \leq 5.06$, respectively.

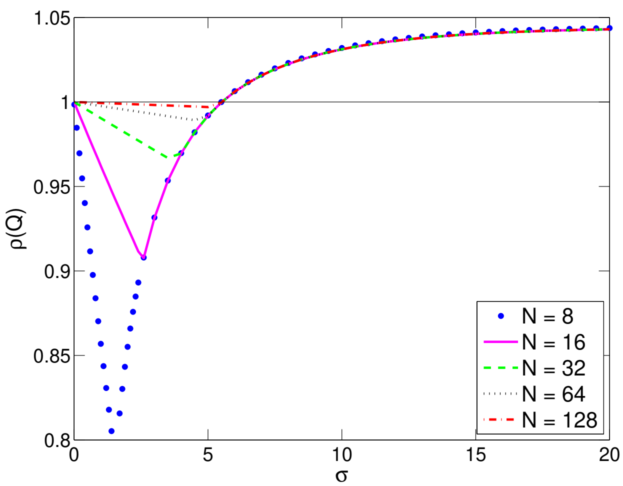

Figure 7: The spectral radii of the iteration matrix for the QSCB-CN method applied to problem (27)-(29).

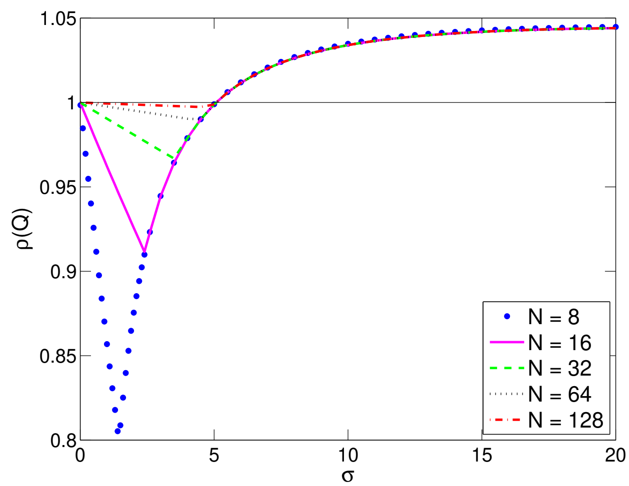

Figure 8: The spectral radii of the iteration matrix for the QSC-CN method applied to problem (27)-(29).

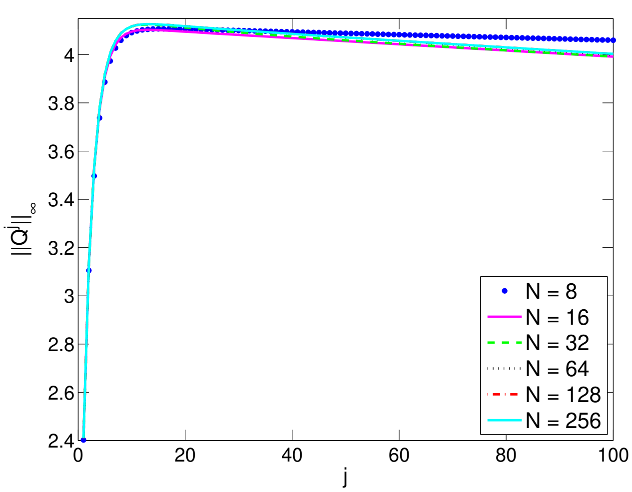

Figure 9: The powers of the iteration matrix for the QSCB-CN method applied to problem (27)-(29); σ=5.5.

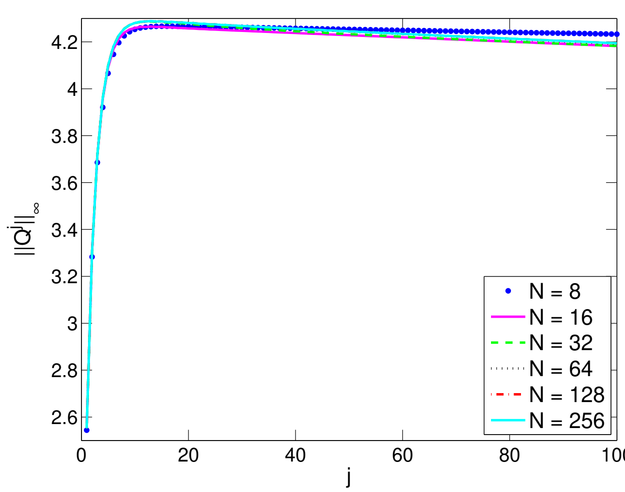

Figure 10: The powers of the iteration matrix for the QSC-CN method applied to problem (27)-(29); σ =5.06.

REMARK 4 From the data plotted in Figures 9 and 10, we have that $\max_{j=0,1,\ldots,T/h_t} ||Q^j||_\infty = ||Q^{13}||_\infty$ for all values of N tested, except for $N = 8$, for which we have $\max_{j=0,1,\ldots,T/h_t} ||Q^j||_\infty = ||Q^{16}||_\infty$. Thus we have $\lim_{h\to 0}(\max_{j=0,1,\ldots,T/h_t} ||Q^j||_\infty) = ||Q^{13}||_\infty$. In Figures 11 and 12, we visualize the boundedness of $||Q||_\infty$ (which implies the boundedness of $||Q^{13}||_\infty$), for the QSCB-CN and QSC-CN methods, respectively. It is worth noting that the boundedness of $||Q||_\infty$ for QSCB-CN and QSC-CN is independent of both N and σ, however, the stability of the methods holds under the above mentioned conditions for σ.

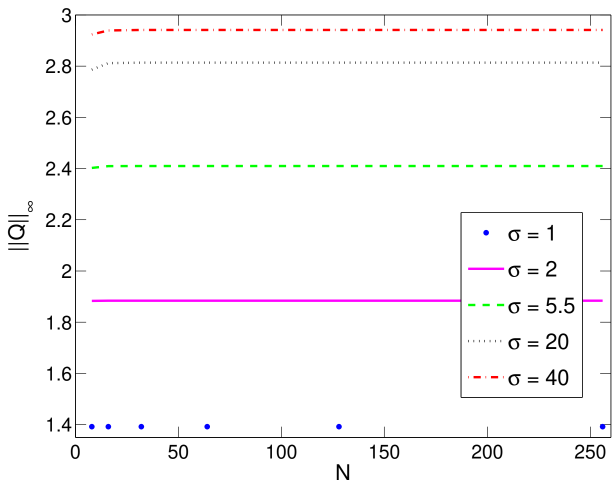

Figure 11: The infinity norm of the iteration matrix for the QSCB-CN method applied to problem (27)-(29).

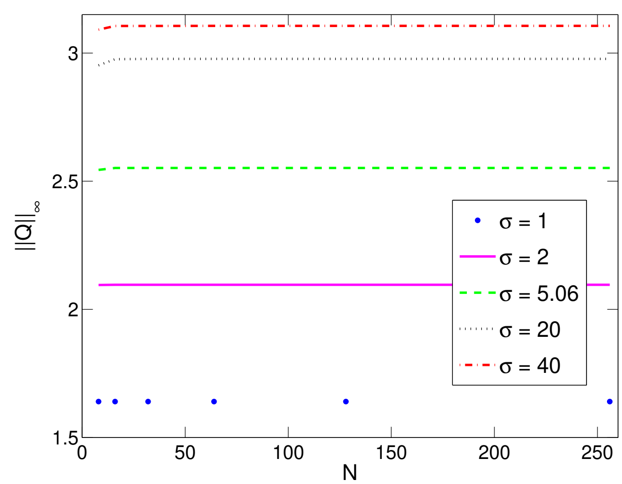

Figure 12: The infinity norm of the iteration matrix for the QSC-CN method applied to problem (27)-(29).

We now study the convergence properties of QSCB-CN. We make use of the following lemma, the proof of which uses the definitions of $\mathcal{P}_\mathcal{L}$, the interpolation relations in [13] and Taylor's expansions, and is omitted for brevity.

LEMMA 2 *If $u^0 \in \mathcal{C}^6[\Omega]$, then*

$$\mathcal{P}_\mathcal{L}(\hat{u}_I^j - \hat{u}_I^{j-1}) = O(h^4 + h_t h^2), \textit{ for } x = \tau_i \textit{ and } j > 0. \tag{69}$$

For later convenience, define

$$R_2^j \equiv \frac{1}{2}\mathcal{P}_\mathcal{L}(\hat{u}_I^j - \hat{u}_I^{j-1}), \tag{70}$$

and notice that, from Lemma 2, we have

$$R_2^j = O(h^4 + h_t h^2), \text{ for } x = \tau_i \text{ and } j > 0. \tag{71}$$

We also use the following lemma, the proof of which is similar to the proof of Lemma 1.

LEMMA 3 *The inverse of matrix A in (66) with A_0 as in (36) and A_σ and B_σ as in (67) exists, and $||A^{-1}||_\infty$ is bounded independently of h.*

THEOREM 3 *If $u^0 \in \mathcal{C}^6[\Omega]$ and $\sigma \leq 5.5$, we have for $j = 0, \ldots, M$,*

$$\begin{aligned}
||(u_\Delta^j)^{(k)} - (u^j)^{(k)}||_\infty &= O(h^{3-k}),\ k = 0, 1, 2\\
|u_\Delta^j(x) - u^j(x)| &= O(h^4), \textit{ for } x = x_i \textit{ and } x = \tau_i\\
|(u_\Delta^j)'(x) - (u^j)'(x)| &= O(h^3), \textit{ for } x = x_i + \lambda h,\ \lambda = (3 \pm \sqrt{3})/6\\
|(u_\Delta^j)''(x) - (u^j)''(x)| &= O(h^2), \textit{ for } x = \tau_i.
\end{aligned}$$

Proof: The proof is similar to the proof of Theorem 2, with a few differences. We prove that at each time step t_j

$$\|(u_\Delta^j)^{(k)} - (\hat{u}_I^j)^{(k)}\|_\infty = t_j O(h^{4-k}),\ k = 0, 1, 2. \tag{72}$$

All the following equations are satisfied at the collocation points τ_i, $i = 1, \dots, N$, unless otherwise indicated. We ignore terms with order higher than $O(h^4)$.
Notice that relations (49)-(51) and (55), used in the proof of Theorem 2, are still valid. Moving the $\frac{1}{2}h_t\mathcal{P}_\mathcal{L}u_I^j$ term in (51) to the right side, and using the definition of R_2^{j-1} in (70), relation (51) is written as

$$\hat{u}_I^j - \frac{1}{2}h_t\mathcal{L}\hat{u}_I^j = \hat{u}_I^{j-1} + \frac{1}{2}h_t(\mathcal{L} + 2\mathcal{P}_\mathcal{L})\hat{u}_I^{j-1} + h_t(R^j + \frac{1}{2}R_1^j + \frac{1}{2}R_1^{j-1} + R_2^j). \tag{73}$$

Define

$$\epsilon^j \equiv R^j + \frac{1}{2}R_1^j + \frac{1}{2}R_1^{j-1} + R_2^j, \tag{74}$$

and notice that, from (40), (47), and (71), we have

$$\epsilon^j = O(h_t^2 + h_t h^2 + h^4), \tag{75}$$

which, by letting $h_t = O(h^2)$, gives

$$\epsilon^j = O(h^4). \tag{76}$$

Relations (73), taking into account (55), after some manipulation, lead to the matrix equations

$$A\vec{\hat{c}}_I^j = B\vec{\hat{c}}_I^{j-1} + h_t\vec{\epsilon}^j + \vec{\zeta}^j, \tag{77}$$

where A and B are given in (66), and $\vec{\zeta}^j$ is a vector with $\zeta_i^j = 0$, for $i = 2, \dots, N-1$, and $\zeta_i^j = O(h^6)$, for $i = 1, N$, i.e.

$$\|\vec{\zeta}^j\|_\infty = O(h^6). \tag{78}$$

Taking into account Lemma 3, the rest of the proof follows with similar arguments as in the proof of Theorem 2. □

Again, note that the technique for proving the convergence orders of QSCB-CN used in Theorem 3 cannot be directly applied to study the convergence of QSC-CN, for reasons similar to those explained in the previous section regarding the convergence of 1QSC-CN. However, as shown in Section 7, all numerical results indicate that, when stability is preserved, the approximation computed by QSC-CN satisfies the same error bounds as the one computed by QSCB-CN, that is, the perturbation $\mathcal{P}_I$ for the boundary equations is needed only for the analysis of the method.

We now discuss further the stepsize restriction of QSCB-CN and QSC-CN. It is somehow expected that the explicit treatment of the term $h_t\lambda\mathcal{P}_\mathcal{L}^j U^j$ of (8) would lead to some stepsize restriction for stability. While a stepsize restriction of the form $\sigma \le 5.5$ is much milder than typical restrictions for explicit methods (e.g. $\sigma \le 0.5$), we will consider techniques to avoid it.

We examined the source of the instability of QSC-CN and QSCB-CN for problem (27)-(29), and we found that it is the perturbation term $\mathcal{P}_\mathcal{L}u_\Delta^{j-1}$ of (9) corresponding to the first and last midpoints (collocation points), namely τ_1 and τ_N, that is responsible for the fact that some eigenvalues of Q may become larger than one in magnitude. We considered some remedies to this issue, such as altering the perturbation term $\mathcal{P}_\mathcal{L}u_\Delta^{j-1}$ at the first and last midpoints. We focus on QSC-CN, but a similar discussion applies to QSCB-CN. One remedy sets the perturbation term $\mathcal{P}_\mathcal{L}u_\Delta^{j-1}$ at the first and last midpoints so that the eigenvalues of Q satisfy certain desirable formulae, giving rise to a method referred to as *QSC-CN2*; another omits this perturbation term completely giving rise to a method referred to as *QSC-CN0*. We also obtain the methods *QSCB-CN2* and *QSCB-CN0* in a similar way. More specifically, methods QSC-CN0 and QSCB-CN0 are described by equations (9) and (26), respectively, with

$$\mathcal{P}_\mathcal{L}u_\Delta(\tau_1) \equiv -\frac{q(\tau_i)}{24}(2u'_\Delta(\tau_1) - 5u'_\Delta(\tau_2) + 4u'_\Delta(\tau_3) - u'_\Delta(\tau_4)) \tag{79}$$

and similarly at $x = \tau_N$, and with $\mathcal{P}_{\mathcal{L}} u_\Delta(\tau_i)$, $i = 2, \ldots, N-1$, as in (10), and $\mathcal{P}_{\mathcal{B}} u_\Delta(x_0)$ as in (12), and similarly at $x = x_N$. Methods QSC-CN2 and QSCB-CN2 are described by equations (9) and (26), respectively, with

$$\mathcal{P}_{\mathcal{L}} u_\Delta(\tau_1) \equiv \frac{p(\tau_i)}{24}(-3u''_\Delta(\tau_1) + u''_\Delta(\tau_2)) - \frac{q(\tau_i)}{24}(2u'_\Delta(\tau_1) - 5u'_\Delta(\tau_2) + 4u'_\Delta(\tau_3) - u'_\Delta(\tau_4)) \tag{80}$$

and similarly at $x = \tau_N$, and with $\mathcal{P}_{\mathcal{L}} u_\Delta(\tau_i)$, $i = 2, \ldots, N-1$, as in (10), and $\mathcal{P}_{\mathcal{B}} u_\Delta(x_0)$ as in (12), and similarly at $x = x_N$. Let

$$A_2 = \begin{bmatrix} -3 & 1 & 0 & 0 & 0\cdots & 0 \\ 1 & -2 & 1 & 0 & 0\cdots & 0 \\ \ddots & \ddots & \ddots & \ddots & \ddots & \ddots \\ 0\cdots & 0 & 0 & 1 & -2 & 1 \\ 0\cdots & 0 & 0 & 0 & 1 & -3 \end{bmatrix}, A_2^0 = \begin{bmatrix} 0 & 0 & 0 & 0 & 0\cdots & 0 \\ 1 & -2 & 1 & 0 & 0\cdots & 0 \\ \ddots & \ddots & \ddots & \ddots & \ddots & \ddots \\ 0\cdots & 0 & 0 & 1 & -2 & 1 \\ 0\cdots & 0 & 0 & 0 & 0 & 0 \end{bmatrix}. \tag{81}$$

For the PDE problem (27)-(29), the QSC-CN2 method gives rise to linear system (34) with

$$A = A_0 - \frac{1}{2}\sigma A_2, \;\; B = A_0 + \frac{1}{2}\sigma A_2 + \frac{1}{24}\sigma (A_2)^2, \tag{82}$$

and the QSC-CN0 method gives rise to linear system (34) with

$$A = A_0 - \frac{1}{2}\sigma A_2, \;\; B = A_0 + \frac{1}{2}\sigma A_2 + \frac{1}{24}\sigma A_2^0 A_2. \tag{83}$$

From [4], we know that the eigenvalues of A_2 are

$$\lambda_i = -4\sin^2(\frac{i\pi}{2N}), \;\; i = 1, \ldots, N, \tag{84}$$

and an orthogonal set of eigenvectors for A_2 is $\{\delta_i\}_{i=1}^N$, with

$$(\delta_i)_j = \kappa_i \sin\frac{(2j-1)i\pi}{2N}, \; j = 1\;, \ldots, N, \;\; \text{with } \kappa_i = 1/2, i = 1, \ldots, N-1, \kappa_N = 1/(2\sqrt{2}). \tag{85}$$

Since $A_0 = \frac{1}{8}(8I + A_2)$, A_0 and A_2 share the same eigenvectors, and the eigenvalues of A_0 are $1 + \frac{1}{8}\lambda_i$. Therefore, $(A_0 - \frac{1}{2}\sigma A_2)^{-1}$ exists and it is easy to see that the eigenvalues of $Q = A^{-1}B$ corresponding to the QSC-CN2 method (with A and B as in (82)) are

$$\mu_i = (1 + \frac{\lambda_i}{8} + \sigma\frac{\lambda_i}{2} + \sigma\frac{(\lambda_i)^2}{24})/(1 + \frac{\lambda_i}{8} - \sigma\frac{\lambda_i}{2}), i = 1, \ldots, N, \tag{86}$$

from which we derive that $|\mu_i| < 1$, therefore $\rho(Q) < 1$. Thus, the QSC-CN2 method the PDE problem (27)-(29) is stable without condition on the time stepsize. In Figure 15, we plot the spectral radii of the QSC-CN2 method applied to the PDE problem (27)-(29) versus σ for different values of N. We see that the spectral radii of QSC-CN2 behave similarly as those of 1QSCB-CN and 1QSC-CN. To study the stability of the QSC-CN0 method, we study how $||Q^j||_\infty$ for the QSC-CN0 method behaves as j increases, for several values of σ and N. Figure 13 shows the results for $\sigma = 20$. Similar behaviour was noted for other values of σ. From the results, we can deduce that $\lim_{h\to 0}(\max_{j=0,1,\ldots,T/h_t} ||Q^j||_\infty) = ||Q||_\infty$, and this quantity is bounded independently of h. Thus, the QSC-CN0 method for the PDE problem (27)-(29) is stable without restriction for the time stepsize.

REMARK 5 In Figure 16, we plot the spectral radii of the QSC-CN0 iteration matrix versus σ for different values of N. From Figures 15 and 16, we notice that the spectral radii of the iteration matrices of QSC-CN2 and QSC-CN0 behave similarly. Moreover, the spectral radii of the QSC-CN2 method are slightly smaller than the respective ones of the QSC-CN0 method, and grow more slowly than those of the QSC-CN0 method as σ increases. Furthermore, the optimal σ that minimizes the spectral radius of the iteration matrix of the QSC-CN2 method is larger than that of the QSC-CN0 method. We may say that the QSC-CN2 method appears to be better than the QSC-CN0 method as far as stability is concerned, however, the simplicity of QSC-CN0 makes it quite attractive. Similar results were obtained for the QSCB-CN2 and QSCB-CN0 methods.

REMARK 6 Using techniques similar to those of the proof of Lemma 1, we can show that the inverse of matrix A in (83) with A_0 as in (36) and A_2 as in (81) exists, and $||A^{-1}||_\infty$ is bounded independently of h. Taking into account this fact and the form of B in (83), we can also easily show that the norm $||Q||_\infty$ of matrix $Q = A^{-1}B$ with A and B as in (83), A_0 as in (36), and A_2 and A_2^0 as in (81) (i.e. Q of QSC-CN0) is bounded independently of h. Figure 14 helps visualize this result. It is worth noting that $||Q||_\infty$ for the 1QSCB-CN, 1QSC-CN, and QSC-CN0 methods first increases with N then reaches its asymptotic bound (around $N = 64$ for $\sigma = 40$), while $||Q||_\infty$ for the QSCB-CN and QSC-CN methods is almost insensitive to N.

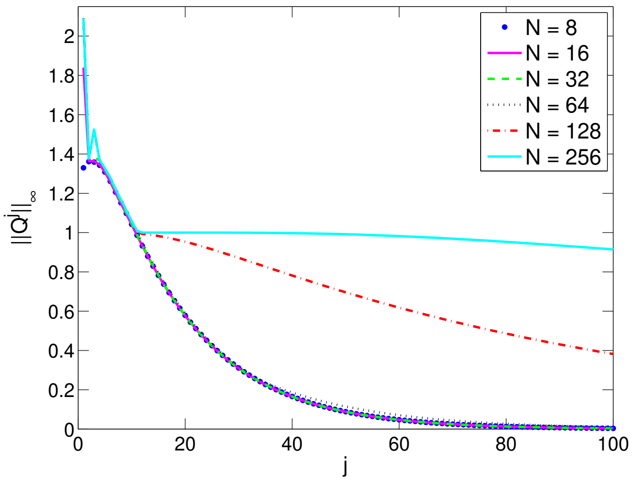

Figure 13: The powers of the iteration matrix for the QSC-CN0 method applied to problem (27)-(29); σ=20.

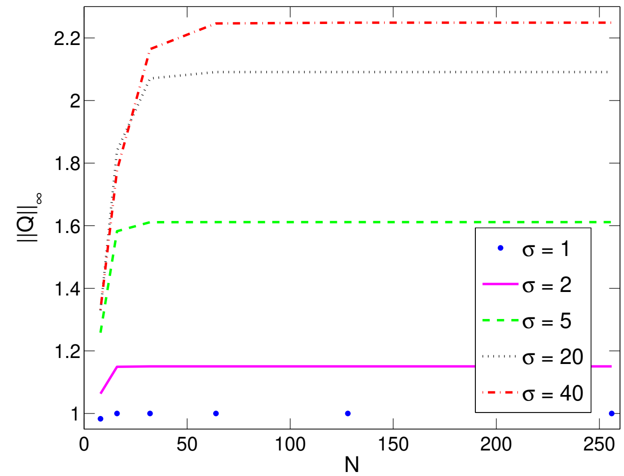

Figure 14: The infinity norm of the iteration matrix for the QSC-CN0 method applied to problem (27)-(29).

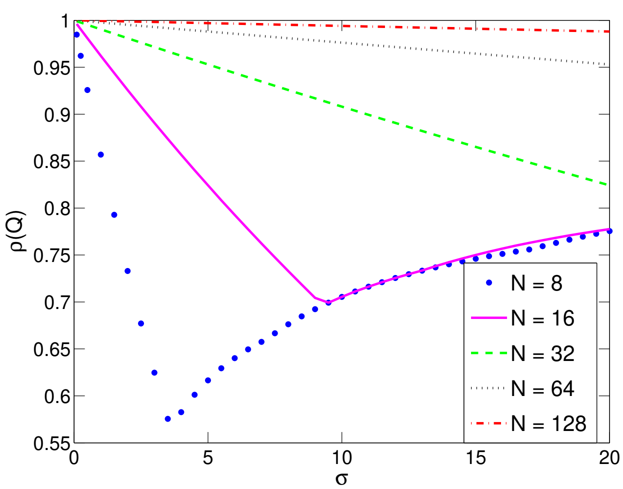

Figure 15: The spectral radii of the iteration matrix for the QSC-CN2 method applied to problem (27)-(29).

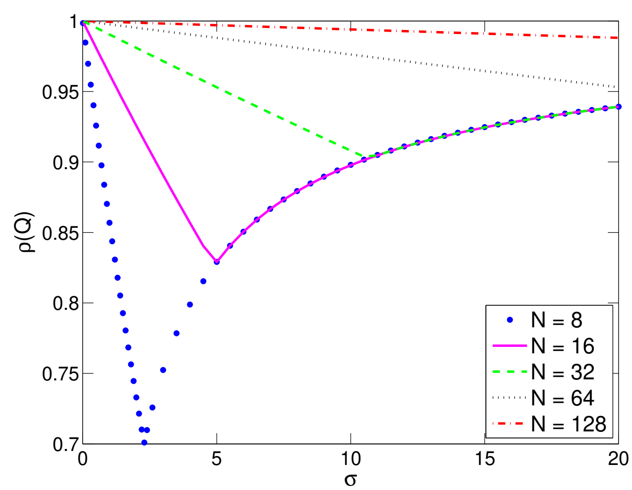

Figure 16: The spectral radii of the iteration matrix for the QSC-CN0 method applied to problem (27)-(29).

One may argue that altering the perturbation term at the points τ_1 and τ_N may have a negative effect in the accuracy of the resulting method. As numerical results in the last section indicate, this is not true; on the contrary, methods QSC-CN2 and QSC-CN0 are at least as accurate as QSC-CN as well as 2QSC-CN and 1QSC-CN. Note that in [1], Archer formulates and analyzes extrapolated cubic-spline methods for parabolic PDEs, using appropriate perturbations to $\mathcal{L}$. However, at the boundary collocation points, while several choices of perturbation terms are considered, Archer makes the simplest choice, which is not to add any perturbation, and proves that the resulting method is $O(h^4)$ accurate in the uniform norm. Though it is not the subject of this paper, we mention that we implemented non-extrapolated one-step cubic-spline collocation methods for parabolic PDEs, along the same lines as QSC-CN and QSC-CN0, and found out that, when the regular perturbation term $\mathcal{P}_\mathcal{L}$ is added to the equations corresponding to the boundary collocation points, the resulting method suffers from instability, while, when no perturbation term $\mathcal{P}_\mathcal{L}$ is added to these equations, stability is preserved.

We conclude this section with a few more remarks. We have shown the convergence (and stability) of QSCB-CN under the assumption that $\sigma \leq 5.5$. It is desirable to have a proof of the optimal orders of convergence for some of the stable variants of QSCB-CN, namely QSCB-CN0 or QSCB-CN2, or the stable variants of QSC-CN, namely QSC-CN0 or QSC-CN2. This would allow us to have these orders with the sole restriction $h_t = O(h^2)$, where the constant in the O-notation can be very large, allowing for large time stepsizes. (The restriction $h_t = O(h^2)$ cannot be further relaxed if the Crank-Nicolson method is used for the time discretization and $O(h^4)$ errors are targeted.) Unfortunately, if we follow a similar proof approach for QSCB-CN0 or QSCB-CN2 as in Theorem 3, two of the terms ϵ^j in (74), namely those arising from the first and last collocation points, are only $O(h^2)$ and not $O(h^4)$, therefore, the proof of the $O(h^4)$ accuracy cannot be obtained through this technique. There is possibly a different approach that proves the optimal order convergence for some of these methods, but we were not able to obtain it at this point. Extensive numerical experiments, some of which are given in Section 7, indicate that QSC-CN0 (as well as QSC-CN2) gives optimal orders of convergence. In general, we believe that, for a parabolic problem and a stable QSC method, altering the perturbation term $\mathcal{P}_\mathcal{L} u_\Delta^{j-1}$ by $O(1)$ at τ_1 and τ_N does not have any negative effect in the order of convergence.

6 Adaptive mesh methods

Recently, quadratic- and cubic-spline collocation methods with optimal order of convergence have been developed on non-uniform grids and integrated with adaptive mesh techniques [6, 5]. We incorporate adaptive mesh techniques in the space discretization of parabolic PDEs. More specifically, at each time step, we incorporate the Algorithm PlaceMap in [5], that uses the error equidistribution principle to move the partition points in order to obtain a better error distribution along the (spatial) domain, and thus a smaller maximum error over the domain. In this paper, we do not include gridsize estimators and changes of the gridsize from timestep to timestep, such as those in [19]. We plan to incorporate the gridsize estimators in [5] into parabolic problems in the near future.

To proceed from t_{j-1} to t_j, we solve (9) using the partition Δ^{j-1} at t_{j-1}, and obtain an approximation to u^j. We apply PlaceMap using the current approximation. If PlaceMap needs to redistribute the partition points, a new partition Δ^j is computed and (9) is re-solved using interpolated values from the previous time step in the right hand side of (9). For efficiency reasons, we allow at most one iteration in Algorithm PlaceMap at each time step. Thus, the grid is gradually re-distributed as time evolves. The algorithm for timestepping from t_{j-1} to t_j using an adaptive mesh technique is summarized as follows:

1. Let $\Delta^j = \Delta^{j-1}$
2. Compute $u^j_{\Delta^j}$ by solving equations (9)
3. Apply PlaceMap (one iteration) to possibly obtain a new Δ^j
4. If Δ^j remains the same, proceed to line 7, else
5. Interpolate $u^{j-1}_{\Delta^{j-1}}$ to obtain $u^{j-1}_{\Delta^j}$
6. Compute $u^j_{\Delta^j}$ by solving equations (9)
7. Proceed to step j

For functions slowly evolving with time, lines 5 and 6 in the above algorithm can be combined in
5-6. Interpolate $u^j_{\Delta^{j-1}}$ to obtain $u^j_{\Delta^j}$

It is important to note that interpolation in line 5 (or 5-6) above takes place on values of $(\mathcal{I} + (1-\lambda)h_t\mathcal{L} + h_t\mathcal{P}_\mathcal{L}))u^{j-1}_{\Delta^{j-1}}$ and not on degrees of freedom corresponding to $u^{j-1}_{\Delta^{j-1}}$.

7 Numerical results

We consider a number of problems and present the maximum errors over the indicated sets of spatial points at the final time $t = T$, for various methods. All methods were implemented in MATLAB. We remark that the matrices A in (34), for which we need to solve at each time step, do not, in general, require pivoting. For example, for the PDE problem (27)-(29), we know from Lemma 1that the matrix A corresponding to the 1QSCB-CN methodis strictly diagonally dominant. Similar lemmata can be easily shown for the respective matrices of the 1QSC-CN, QSCB-CN and QSC-CN0 methods. For more general PDE problems, we noticed numerically that the matrices A are usually diagonally dominant, and even if they are not, they tend to be so as N increases.

We first consider a model problem to compare the stability and convergence of QSC-CN, QSCB-CN, QSC-CN0, QSC-CN2, 1QSC-CN, 1QSCB-CN and 2QSC-CN.

Problem 1

$$u_t - pu_{xx} = g \quad \text{in} \quad (0,1) \times (0,1) \tag{87}$$

$$u = \gamma \quad \text{on} \quad \{0,1\} \times (0,1) \tag{88}$$

$$u = u^0 \quad \text{on} \quad [0,1] \times \{0\}. \tag{89}$$

Here, $p = 1$, and g, γ and u^0 are chosen so that the exact solution is $u(x,t) = \sin(\pi x)\exp(-t)$. In Table 4, we present indicative results that verify the unconditional stability of QSC-CN0, QSC-CN2, 1QSC-CN, 1QSCB-CN and 2QSC-CN, and the conditional stability of QSC-CN and QSCB-CN for the PDE problem (87)-(89). For QSC-CN, notice that, the more σ is above 5.06, the smaller the gridsize for which the solution blows up. Similarly for QSCB-CN and σ above 5.5. It is worth noting that the results of QSC-CN with $\sigma = 5.06, 5.1, 5.2$ are almost identical with those of QSCB-CN with $\sigma = 5.5, 5.55, 5.65$, respectively. Also, the results of QSC-CN0 and QSC-CN2 are identical, and so are the results of 1QSC-CN and 1QSCB-CN, while the results of 2QSC-CN are almost identical to those of 1QSC-CN. For QSC-CN0, QSC-CN2, 1QSC-CN, 1QSCB-CN and 2QSC-CN, the solution remains bounded and exhibits optimal orders of convergence even for large values of σ. Notice also that QSC-CN and QSC-CN0 give almost identical results, when $\sigma = 5.06$ and $\sigma = 20$, respectively. In these cases, it is the spatial error that dominates, and since both methods are stable, they behave similarly. (The temporal error dominates when σ becomes larger.) Furthermore, QSC-CN0 (and QSC-CN whenever it is stable) are a little more accurate than 1QSC-CN, 1QSCB-CN and 2QSC-CN, possibly because QSC-CN0 (and QSC-CN) do about half the operations of 1QSC-CN, 1QSCB-CN and 2QSC-CN. Taking these results into account, we can say that QSC-CN0 (and QSC-CN2) is at least twice more efficient than 1QSC-CN, 1QSCB-CN and 2QSC-CN. We also note that methods QSCB-CN0 and QSCB-CN2 gave almost identical results to QSC-CN0 and QSC-CN2, but due to space limitations we do not show them.

We next consider a problem with variable coefficients and all terms of $\mathcal{L}u$ nonzero to demonstrate the optimal orders of convergence of QSC-CN0, 1QSC-CN and 2QSC-CN.

Problem 2

$$u_t - pu_{xx} - qu_x + ru = g \quad \text{in} \quad (0,1) \times (0,1) \tag{90}$$

$$u = \gamma \quad \text{on} \quad \{0,1\} \times (0,1) \tag{91}$$

$$u = u^0 \quad \text{on} \quad [0,1] \times \{0\}. \tag{92}$$

Here, $p = 1 + \sin(xt)$, $q = (1 + x^2)/(1 + t)$, $r = x/(1 + x^2)\exp(-t)$, and g, γ and u^0 are chosen so that the exact solution is $u(x,t) = x^{9/2}\exp(-t)$. Table 5 shows the results. By $||\cdot||_{x_i}$, $||\cdot||_{\tau_i}$, $||\cdot||_\infty$ and $||\cdot||_{\delta_i}$, we denote the errors at the gridpoints, midpoints, a set of 1000 uniform points, and the Gauss points of each subinterval, respectively. The error at a set of 1000 uniform points is taken as an approximation to the uniform norm of the error. For this problem, the value of σ varies with x and t, since p varies. More specifically, σ ranged from about 80 to about 147. We notice that all three methods (QSC-CN0, 1QSC-CN and 2QSC-CN) exhibit optimal orders of convergence, equivalent to those exhibited by the optimal QSC methods in [13] for BVPs. The errors of 1QSC-CN

Table 4: Observed errors on the gridpoints and respective orders of convergence by the QSC-CN, QSC-CN0 and 2QSC-CN methods for Problem 1 with $p = 1$, for several gridsizes N and choices of σ.

N	error	order	error	order	error	order
	QSC-CN/QSCB-CN					
	$\sigma = 5.06/5.5$		$\sigma = 5.1/5.55$		$\sigma = 5.2/5.65$	
16	1.2e-05		1.2e-05		1.2e-05	
32	7.3e-07	4.00	7.3e-07	4.00	7.3e-07	4.00
64	4.5e-08	4.00	4.5e-08	4.00	4.5e-08	4.00
128	2.8e-09	4.00	2.8e-09	4.00	2.8e-09	4.00
256	1.8e-10	4.00	1.8e-10	4.00	2.4e-06 [1]	-9.75
512	1.1e-11	4.01	2.0e-07 [1]	-10.14		
	QSC-CN0 and QSC-CN2					
	$\sigma = 20$		$\sigma = 40$		$\sigma = 80$	
16	1.2e-05		2.0e-05		1.4e-04	
32	7.3e-07	4.00	1.9e-06	3.39	1.2e-05	3.49
64	4.5e-08	4.00	1.4e-07	3.80	9.0e-07	3.76
128	2.8e-09	4.00	8.9e-09	3.97	5.7e-08	3.97
256	1.8e-10	4.00	5.6e-10	3.99	3.6e-09	3.98
512	1.1e-11	4.00	3.6e-11	3.97	2.3e-10	4.00
	1QSC-CN and 1QSCB-CN					
	$\sigma = 20$		$\sigma = 40$		$\sigma = 80$	
16	2.2e-05		5.7e-05		2.0e-04	
32	1.5e-06	3.82	4.9e-06	3.55	1.8e-05	3.49
64	9.6e-08	3.97	3.4e-07	3.86	1.3e-06	3.80
128	6.1e-09	3.99	2.1e-08	3.97	8.2e-08	3.97
256	3.8e-10	4.00	1.3e-09	3.99	5.2e-09	3.99
512	2.3e-11	4.06	8.3e-11	4.04	3.2e-10	4.01
	2QSC-CN					
	$\sigma = 20$		$\sigma = 40$		$\sigma = 80$	
16	2.2e-05		5.8e-05		2.0e-04	
32	1.5e-06	3.85	4.9e-06	3.56	1.8e-05	3.49
64	9.7e-08	3.98	3.4e-07	3.87	1.3e-06	3.80
128	6.1e-09	3.99	2.1e-08	3.97	8.2e-08	3.97
256	3.8e-10	4.00	1.3e-09	3.99	5.2e-09	3.99
512	2.4e-11	3.99	8.5e-11	3.98	3.3e-10	4.00

and 2QSC-CN are almost identical and about equivalent to those of QSC-CN0, therefore QSC-CN0 is about twice as efficient as 1QSC-CN and 2QSC-CN. We also notice that, although u has only four bounded derivatives with respect to x in $[0, 1]$, the optimal orders still hold. This fact indicates that the assumption $u^0 \in \mathcal{C}^6[\Omega]$ is sufficient for the results of Section 7, but not necessary. With additional results on a problem similar to Problem 2, but with $u(x, t) = x^{7/2} \exp(-t)$ [3], which gave slightly reduced orders of convergence, we conclude that $u^0 \in \mathcal{C}^4[\Omega]$ is necessary and sufficient to obtain the optimal orders of convergence.

We next consider a problem with mixed boundary conditions.

[1] For QSCB-CN, with $N = 512$ and $\sigma = 5.55$, the error is 8.3e-09, and with $N = 256$ and $\sigma = 5.65$, the error is 6.22e-08.

Table 5: Observed errors at the indicated sets of points and respective orders of convergence by the QSC-CN0, 1QSC-CN and 2QSC-CN methods for Problem 2, for several gridsizes N, with $h_t = 80h_x^2$.

	$\|\|u-u_\Delta\|\|_{x_i}$		$\|\|u-u_\Delta\|\|_{\tau_i}$		$\|\|u-u_\Delta\|\|_\infty$		$\|\|\frac{\partial(u-u_\Delta)}{\partial x}\|\|_{\delta_i}$		$\|\|\frac{\partial^2(u-u_\Delta)}{\partial x^2}\|\|_{\tau_i}$	
N	error	order	error	order	error	order	error	order	error	order
	QSC-CN0									
16	1.7e-05		1.9e-05		7.7e-05		3.3e-04		1.0e-02	
32	1.9e-06	3.21	2.0e-06	3.27	9.6e-06	3.00	3.4e-05	3.30	2.6e-03	1.97
64	1.2e-07	3.98	1.2e-07	3.98	1.2e-06	3.01	4.2e-06	2.99	6.6e-04	1.98
128	7.6e-09	3.95	8.0e-09	3.95	1.5e-07	3.00	5.3e-07	3.00	1.7e-04	1.99
256	4.8e-10	3.99	5.1e-10	3.99	1.9e-08	3.00	6.6e-08	3.00	4.1e-05	2.00
512	3.0e-11	4.00	3.2e-11	4.00	2.3e-09	3.03	8.3e-09	3.00	1.0e-05	2.00
	1QSC-CN									
16	1.8e-05		1.6e-05		7.7e-05		2.7e-04		1.0e-02	
32	1.6e-06	3.54	1.4e-06	3.51	9.6e-06	3.00	3.4e-05	2.98	2.6e-03	1.97
64	1.2e-07	3.68	1.1e-07	3.66	1.2e-06	3.01	4.2e-06	2.99	6.6e-04	1.98
128	7.9e-09	3.95	7.4e-09	3.95	1.5e-07	3.00	5.3e-07	3.00	1.7e-04	1.99
256	5.0e-10	3.97	4.7e-10	3.97	1.9e-08	3.00	6.6e-08	3.00	4.1e-05	2.00
512	3.1e-11	4.00	2.9e-11	4.00	2.3e-09	3.03	8.3e-09	3.00	1.0e-05	2.00
	2QSC-CN									
16	1.8e-05		1.6e-05		7.7e-05		2.7e-04		1.0e-02	
32	1.6e-06	3.55	1.4e-06	3.52	9.6e-06	3.00	3.4e-05	2.99	2.6e-03	1.97
64	1.2e-07	3.69	1.1e-07	3.67	1.2e-06	3.01	4.2e-06	2.99	6.6e-04	1.98
128	7.8e-09	3.95	7.3e-09	3.95	1.5e-07	3.00	5.3e-07	3.00	1.7e-04	1.99
256	5.0e-10	3.97	4.6e-10	3.97	1.9e-08	3.00	6.6e-08	3.00	4.1e-05	2.00
512	3.1e-11	4.00	2.9e-11	4.00	2.3e-09	3.03	8.3e-09	3.00	1.0e-05	2.00

Problem 3

$$u_t - pu_{xx} - qu_x + ru = g \quad \text{in} \quad (0,1)\times(0,1) \tag{93}$$

$$u + u_{\mathrm{n}} = \gamma \quad \text{on} \quad \{0,1\}\times(0,1) \tag{94}$$

$$u = u^0 \quad \text{on} \quad [0,1]\times\{0\}. \tag{95}$$

Here, p, q, r are as in Problem 2, u_{n} denotes the normal derivative of u in the space variable, and g, γ and u^0 are chosen so that the exact solution is $u(x,t) = \exp(x+t)$. Table 6 shows the results. We notice that QSC-CN0, 1QSC-CN and 2QSC-CN exhibit optimal orders, and give quite similar results.

We now turn to convection-dominated problems and consider the QSC-CN, QSC-CN0, 1QSC-CN and 2QSC-CN methods. The case of convection-dominated problems needs to be dealt carefully, since quadratic splines require a perturbation for the term qu_x of $\mathcal{L}$ in order to reach the optimal order of convergence.

Problem 4

$$u_t - pu_{xx} - qu_x = g \quad \text{in} \quad (0,1)\times(0,1) \tag{96}$$

$$u = \gamma \quad \text{on} \quad \{0,1\}\times(0,1) \tag{97}$$

$$u = u^0 \quad \text{on} \quad [0,1]\times\{0\}. \tag{98}$$

We first pick $p = 0.1$, $q = 100$, and g, γ and u^0 so that the exact solution is $u(x,t) = \exp(x+t)$. Table 7 shows the results with $\sigma = 0.1$, which results in $h_t = h^2$. We first notice that the 1QSC-CN method is the most accurate for this problem. We also notice that the 2QSC-CN method gives reasonable and decreasing errors for all

Table 6: Observed errors at the indicated sets of points and respective orders of convergence by the QSC-CN0, 1QSC-CN and 2QSC-CN methods for Problem 3, for several gridsizes N, with $h_t = 80h_x^2$.

	$\|\|u - u_\Delta\|\|_{x_i}$		$\|\|u - u_\Delta\|\|_{\tau_i}$		$\|\|u - u_\Delta\|\|_\infty$		$\|\|\frac{\partial(u-u_\Delta)}{\partial x}\|\|_{\delta_i}$		$\|\|\frac{\partial^2(u-u_\Delta)}{\partial x^2}\|\|_{\tau_i}$	
N	error	order	error	order	error	order	error	order	error	order
	QSC-CN0									
16	1.0e-02		1.0e-02		1.0e-02		7.9e-03		1.8e-02	
32	7.1e-04	3.82	7.1e-04	3.82	7.1e-04	3.82	5.7e-04	3.81	1.4e-03	3.73
64	4.7e-05	3.93	4.7e-05	3.93	4.7e-05	3.92	3.8e-05	3.90	1.7e-04	3.00
128	2.9e-06	4.01	2.9e-06	4.01	2.9e-06	4.01	2.4e-06	4.00	2.5e-05	2.80
256	1.8e-07	4.04	1.8e-07	4.04	1.8e-07	4.03	1.6e-07	3.87	5.6e-06	2.15
512	1.0e-08	4.09	1.0e-08	4.09	1.1e-08	4.07	1.1e-08	3.91	1.3e-06	2.17
	1QSC-CN									
16	9.9e-03		9.9e-03		9.9e-03		7.9e-03		1.9e-02	
32	7.0e-04	3.82	7.0e-04	3.82	7.0e-04	3.81	5.6e-04	3.82	1.4e-03	3.77
64	4.6e-05	3.92	4.6e-05	3.92	4.7e-05	3.91	3.8e-05	3.88	1.5e-04	3.20
128	2.9e-06	3.99	2.9e-06	3.99	2.9e-06	3.98	2.4e-06	3.96	2.4e-05	2.66
256	1.8e-07	3.99	1.8e-07	3.99	1.9e-07	3.99	1.6e-07	3.96	5.0e-06	2.25
512	1.2e-08	3.99	1.2e-08	3.99	1.2e-08	3.98	1.0e-08	3.93	1.2e-06	2.07
	2QSC-CN									
16	9.9e-03		9.9e-03		9.9e-03		7.8e-03		1.9e-02	
32	7.0e-04	3.82	7.0e-04	3.82	7.0e-04	3.81	5.6e-04	3.82	1.4e-03	3.77
64	4.6e-05	3.92	4.6e-05	3.92	4.7e-05	3.92	3.8e-05	3.86	1.6e-04	3.14
128	2.9e-06	3.99	2.9e-06	3.99	2.9e-06	3.99	2.5e-06	3.96	2.4e-05	2.69
256	1.8e-07	4.00	1.8e-07	4.00	1.8e-07	4.00	2.0e-07	3.63	7.9e-06	1.62
512	1.1e-08	4.04	1.1e-08	4.04	1.1e-08	4.02	1.3e-08	3.98	1.3e-06	2.58

N and the respective h_t, while the QSC-CN and QSC-CN0 methods give huge and increasing errors for small N ($N < 64$), and, therefore, large h_t. These numerical experiments, indicate that 1QSC-CN and 2QSC-CN are stable and convergent even for large h_t, while the QSC-CN and QSC-CN0 methods are stable and convergent when h_t is small enough. Furthermore, when h_t is small enough so that the QSC-CN and QSC-CN0 methods are stable and convergent, both methods are more accurate than 2QSC-CN, with the QSC-CN0 method being the most accurate, with errors just slightly larger than those of 1QSC-CN. We investigated this issue further, and attempted to find numerically the problem parameters and the relations they need to satisfy, in order for the QSC-CN and QSC-CN0 methods to be stable and convergent for convection-dominated problems. The parameters we considered are h_t, N, p, q, as well as the length L of the spatial domain. Through several experiments, we found that h_t must satisfy the relation

$$h_t \leq c\frac{p}{q^2}, \tag{99}$$

where c is a constant, with $c \approx 25$. The relation (99) seems to be a sufficient condition for the QSC-CN0 method to be stable and convergent. The same holds for QSC-CN (if, in addition, $\sigma \leq 5.06$).

To support our argument, we solve Problem 4 for various values of the parameters h_t, N, p, q and L, and present selected results. We focus on the QSC-CN0 method, since this method does not have a stepsize restriction for the plain diffusion problems, and seems more accurate for convection-dominated problems. To find the relation h_t should satisfy, we pick certain values for N, p, q and L, and compute the solution of Problem 4 by the QSC-

Table 7: Errors of the QSC-CN, QSC-CN0, 2QSC-CN and 1QSC-CN methods for Problem 4, with $p = 0.1$, $q = 100$, and $\sigma = 0.1$.

N	$\|u - u_\Delta\|_{x_i,\tau_i,\infty}$											
	QSC-CN			QSC-CN0			2QSC-CN			1QSC-CN		
16	1.3+44	2.5+44	2.6+44	1.5+30	1.6+30	1.8+30	1.8-04	1.6-03	1.6-03	4.3-07	1.9-06	1.5-05
32	4.7+76	6.8+76	7.1+76	3.0+66	3.0+66	3.3+66	6.0-06	4.1-05	4.1-05	2.3-08	6.1-08	1.8-06
64	5.7-09	1.1-08	2.3-07	4.6-09	1.0-08	2.2-07	1.9-07	6.9-07	7.0-07	1.5-09	3.6-09	2.3-07
128	3.4-10	4.7-10	2.8-08	1.9-10	2.8-10	2.8-08	9.4-09	1.3-08	3.4-08	9.2-11	2.2-10	2.8-08

CN0 method with several values of h_t, and try to determine the maximum h_t for which the method is stable and convergent. Clearly, we could not test all possible values of h_t, but, for each set of values for N, p, q and L, we started the tests with some value of h_t that gave reasonable results, then increased h_t by increments of half an order of magnitude, up to the point the errors started becoming huge and, therefore, unacceptable. In Table 8, we present the maximum h_t, calculated as described above, and the associated errors.

The first four rows of Table 8 have N, q, L fixed and p varying. The next three rows have N, p, L fixed and q varying. The next four rows have p, q, L fixed and N varying. The last three rows have N, p, q fixed and L varying. These experiments indicate that the maximum h_t for which the QSC-CN method is stable and convergent depends approximately linearly to p, inversely to q^2, and does not depend on N and L. Clearly, relation (99) seems to hold with remarkable accuracy. We included the value of $25\frac{p}{q^2}$ in the table, to emphasize how well the numerically calculated maximum h_t agrees with $25\frac{p}{q^2}$. There are a few cases (rows 1, 3 and 7 in Table 8) in which we found a h_t slightly larger than $25\frac{p}{q^2}$, that results in a stable and convergent method. In all other cases, we have full agreement between the maximum h_t and $25\frac{p}{q^2}$.

As mentioned before, we also implemented cubic-spline collocation methods for parabolic PDEs, along the same lines as QSC-CN and QSC-CN0. Preliminary numerical experiments indicate that the resulting cubic-spline methods do not have a stability condition similar to (99) for convection-dominated problems. However, the study of cubic-spline collocation methods for parabolic PDEs will be the subject of future work.

Problem 5

We considered the American put option pricing problem, and applied the adaptive mesh QSC-CN0 method to it. Under the Black-Scholes framework, with appropriate initial and boundary conditions, together with additional constraints that involve a free boundary, the American put option pricing problem is modelled as a linear complimentarity problem (LCP). We solve the LCP by a penalty method [11], which essentially replaces the LCP by the nonlinear PDE $v_t - \mathcal{L}v = \hat{\rho}\max\{f - v, 0\}$, where $\mathcal{L}v \equiv \frac{\hat{\sigma}^2 S^2}{2} v_{SS} + \hat{r} S v_S - \hat{r} v$, with $\hat{\sigma}$ being the volatility, $\hat{r}$ the risk-free rate, $f = \max\{E - S, 0\}$ the payoff function (also initial state), E the strike price, S the asset price that plays the role of the space variable, and $\hat{\rho}$ a large number (penalty parameter). In the example chosen, $E = 100$, $\hat{\sigma} = 0.80$, $\hat{r} = 0.10$, $T = 0.25$, $\hat{\rho} = 10^7$, and the semi-infinite domain is truncated to $[0, 500]$.

The difficulty in solving this problem arises primarily from the discontinuity of the initial solution at the strike price (the first derivative is discontinuous), and subsequent discontinuities of the second derivative of the solution at the (unknown) free boundary at each t. To better handle the discontinuity in the initial solution, we use the Rannacher smoothing technique [17], which applies a fully-implicit timestepping in the first few (usually two) time steps. In Figure 17, we show the location of the partition points (we show every second partition point, to keep the figure clearer) at selected time steps, as computed by the adaptive algorithm, for the case $N = 135$, $M = 130$. We start with a uniform grid (as if we do not know how the solution behaves). At the first time step, the points are concentrated around the strike. As the time evolves, the points spread to cover the interval between the free boundary (which moves from E to the left) and E, with concentration around the free boundary. Almost no points

Table 8: The maximum h_t which makes the QSC-CN0 method stable and convergent for Problem 4, for the indicated values of N, p, q and L. The respective errors are also shown.

L	N	p	q	$25\frac{p}{q^2}$	h_t	$\|u - u_\Delta\|_{x_i,\tau_i,\infty}$		
1	16	0.1	100	0.00025	0.0003	3.6-07	1.8-06	1.5-05
1	16	1	100	0.0025	0.0025	3.6-07	6.1-07	1.5-05
1	16	2	100	0.005	0.0055	9.4-07	1.3-06	1.4-05
1	16	4	100	0.01	0.01	9.4-06	8.4-06	1.5-05
1	16	1	50	0.01	0.01	3.1-06	3.3-06	1.4-05
1	16	1	100	0.0025	0.0025	3.6-07	6.1-07	1.5-05
1	16	1	200	0.000625	0.000675	3.6-07	7.9-07	1.5-05
1	4	1	100	0.0025	0.0025	2.6-02	3.0-02	3.0-02
1	8	1	100	0.0025	0.0025	5.5-06	1.5-05	1.2-04
1	16	1	100	0.0025	0.0025	3.6-07	6.1-07	1.5-05
1	32	1	100	0.0025	0.0025	1.7-07	1.9-07	1.8-06
1	16	1	50	0.01	0.01	3.1-06	3.3-06	1.4-05
2	16	1	50	0.01	0.01	3.3-05	4.4-05	3.2-04
4	16	1	50	0.01	0.01	2.2-03	5.6-03	2.0-02

are needed to the left of the free boundary (where the solution is linear) and few points are needed towards the right end of the interval, where the solution is almost linear. These results indicate that the adaptive technique correctly captures the behaviour of the solution, and places more points around the discontinuity points.

We next compile a performance comparison between a number of methods for solving this problem. For the time discretization all methods use Crank-Nicolson, with Rannacher smoothing. The methods differ primarily in the space discretization. We consider the uniform second-order FD (uniform FD) method, the non-uniform finite volume method of [11] that uses a certain predetermined distribution of the spatial points, the adaptive mesh FD method in [7] (adaptive FD) that uses a similar timestepping algorithm as the one in Section 6, the control variate method of [15] (control variate), and the adaptive mesh QSC-CN0 method (adaptive QSC) of this paper. Excluding the control variate method, all other methods use the penalty method [11] to handle the free-boundary. In Figure 18, we plot the progress of the computed option value at the strike price, as the number of partition points and time steps increases. Since each method, at each time step (and penalty iteration, if any) solves a tridiagonal linear system of size N, the cost of the method is proportional to N and the total number of iterations (or time steps if no penalty iterations). Figure 18 shows that the QSC-CN0 adaptive mesh method outperforms the adaptive mesh FD method, the non-uniform FD method of [11], as well as other methods. The "exact" value was computed by the data in [11] and extrapolation. The data used for the plot corresponding to the non-uniform FD method in [11] are taken directly from [11] (Table 4, implicit constraint, volatility $= 0.80$), while the other methods are implemented by us.

8 Conclusions and remarks

We have formulated a number of new methods for solving parabolic PDEs. The time discretization is handled by finite differences (primarily Crank-Nicolson), and the space discretization by quadratic-spline collocation. The main computational requirement at each timestep of the extrapolated methods 1QSC-CN and 1QSCB-CN is the solution of one pentadiagonal linear system, of the deferred-correction methods 2QSC-CN and 2QSCB-CN the solution of two tridiagonal linear systems, and of the methods QSC-CN, QSCB-CN, QSC-CN0, QSCB-CN0, QSC-

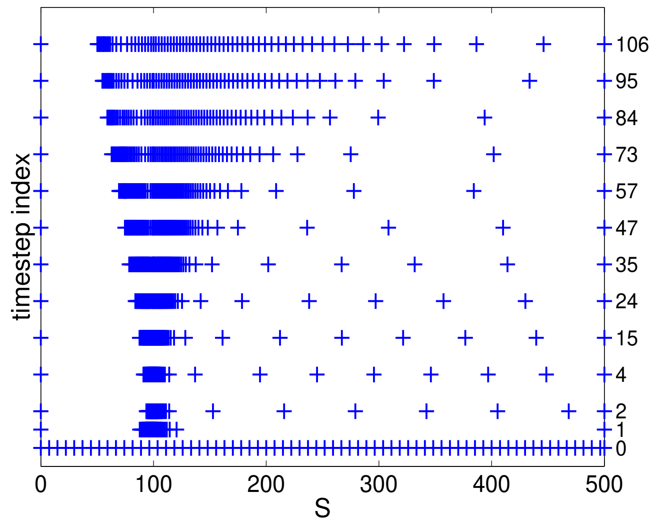

Figure 17: The location of the gridpoints chosen by the adaptive mesh QSC-CN0 method applied to the American put option pricing problem.

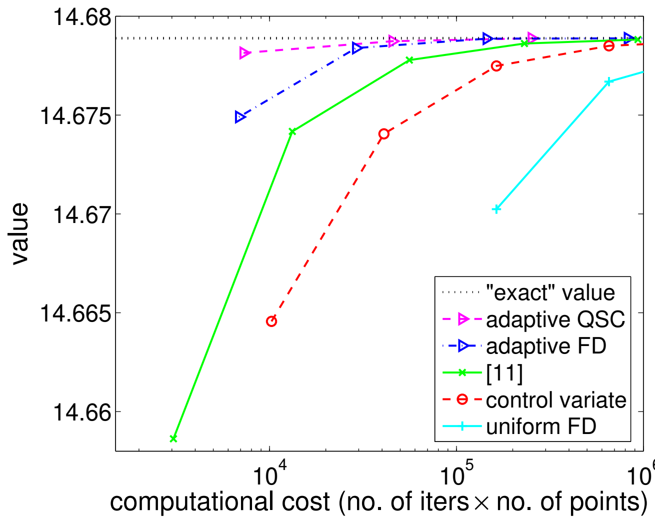

Figure 18: Performance of various methods applied to the American put option pricing problem.

CN2 and QSCB-CN2 the solution of one tridiagonal linear system. Note that the "B" methods (1QSCB-CN, QSCB-CN) differ from their "non-B" counterparts only in an $O(h^4)$ perturbation term ($\mathcal{P}_I$) at the boundary points. This perturbation facilitates the analysis of the convergence of certain methods, while it adds only a small constant amount of work to the methods.

We analyzed some of the new methods, namely methods 1QSCB-CN and QSCB-CN, with respect to stability and convergence for the model heat equation. We found that 1QSCB-CN does not have a time stepsize restriction, while QSCB-CN does. Both methods exhibit optimal orders of convergence, similar to those exhibited by QSC methods for BVPs. For several problems more general than the analysis assumes, numerical experiments indicate that 1QSCB-CN and QSCB-CN still exhibit optimal orders of convergence. Also, numerical experiments indicate that 1QSC-CN gives equivalent results to 1QSCB-CN, and that QSC-CN behaves quite similarly to QSCB-CN.

Methods QSC-CN0, QSC-CN2, QSCB-CN0 and QSCB-CN2 do not have a time stepsize restriction for the model heat equation, and are offered as alternatives to QSCB-CN (and QSC-CN). However, the mathematical analysis of the convergence orders of these methods remains an open problem. Numerical results indicate that the methods exhibit optimal orders of convergence. It should also be noted that these four methods have almost the same computational requirements. For convection-dominated problems, QSC-CN0 has a time stepsize restriction, which seems to be independent of the space stepsize and dependent only on the problem. To conclude, in an error versus computational time comparison, the most efficient method seems to be QSC-CN0 which for most problems requires about half the time of 1QSC-CN, 1QSCB-CN, 2QSC-CN and 2QSCB-CN, while it gives the same accuracy, with the exception of the case of convection-dominated problems when the time stepsize needs to be large. For such problems, 1QSC-CN and 1QSCB-CN seem to be the most effective methods. We believe that the efficiency advantage of QSC-CN0 over 1QSC-CN and 1QSCB-CN will become more evident when the method is extended to two (or more) space dimensions, where we expect QSC-CN0 to require the solution of one block-tridiagonal linear system at each timestep, while, 1QSC-CN and 1QSCB-CN will require the solution of one block-pentadiagonal linear system at each timestep.

References

[1] D. ARCHER, *An $O(h^4)$ cubic spline collocation method for quasilinear parabolic equations*, SIAM J. Numer. Anal., 14 (1977), pp. 620–637.

[2] B. BIALECKI AND G. FAIRWEATHER, *Orthogonal spline collocation methods for partial differential equations*, J. Comput. Appl. Math., 128 (2001), pp. 55–82. Numerical analysis 2000, Vol. VII, Partial differential equations.

[3] T. CHEN, *An efficient algorithm based on quadratic spline collocation and finite difference methods for parabolic partial differential equations*, Master's thesis, University of Toronto, Toronto, Ontario, Canada, 2005.

[4] C. C. CHRISTARA, *Quadratic spline collocation methods for elliptic partial differential equations*, BIT, 34 (1994), pp. 33–61.

[5] C. C. CHRISTARA AND K. S. NG, *Adaptive techniques for spline collocation*, Computing, 76 (2006), pp. 259 – 277.

[6] ——, *Optimal quadratic and cubic spline collocation on nonuniform partitions*, Computing, 76 (2006), pp. 227 – 257.

[7] D. M. DANG, *Adaptive finite difference methods for valuing American options*, Master's thesis, University of Toronto, Toronto, Ontario, Canada, 2007.

[8] C. DE BOOR AND B. SWARTZ, *Collocation at Gaussian points*, SIAM J. Numer. Anal., 10 (1973), pp. 582–606.

[9] J. DOUGLAS AND T. DUPONT, *A finite element collocation method for quasilinear parabolic equations*, Math. Comp., 27 (1973), pp. 17–28.

[10] ——, *Collocation methods for parabolic equations in a single-space variable*, Lecture Notes in Mathematics, 385 (1974), pp. 1–147.

[11] P. A. FORSYTH AND K. VETZAL, *Quadratic convergence for valuing American options using a penalty method*, SIAM J. Sci. Comput., 23 (2002), pp. 2095–2122.

[12] C. E. GREENWELL-YANIK AND G. FAIRWEATHER, *Analyses of spline collocation methods for parabolic and hyperbolic problems in two space variables*, SIAM J. Numer. Anal., 23 (1986), pp. 282–296.

[13] E. N. HOUSTIS, C. C. CHRISTARA, AND J. R. RICE, *Quadratic-spline collocation methods for two-point boundary value problems*, Internat. J. Numer. Methods Engrg., 26 (1988), pp. 935–952.

[14] E. N. HOUSTIS, J. R. RICE, C. C. CHRISTARA, AND E. A. VAVALIS, *Performance of scientific software*, The IMA Volumes in Mathematics and its applications, 14 (1988), pp. 123–155. Mathematical Aspects of Scientific Software, J. R. Rice, ed.

[15] J. C. HULL, *Options, Futures, and Other Derivatives*, Prentice Hall, sixth ed., 2006.

[16] A. ISERLES, *A first Course in the Numerical Analysis of Differential Equations*, Cambridge, 1997.

[17] R. RANNACHER, *Finite element solution of diffusion problems with irregular data*, Numerische Mathematik, 43 (1984), pp. 309–327.

[18] R. WANG, P. KEAST, AND P. MUIR, *BACOL: B-Spline Adaptive COLlocation software for 1-D parabolic PDEs*, ACM Trans. Math. Soft., 30 (2004), pp. 454–470.

[19] ——, *A high-order global spatially adaptive collocation method for 1-D parabolic PDEs*, Applied Numerical Mathematics, 50 (2004), pp. 239–260.

9 Appendix

In the appendix, we present additional data regarding the spectral radii of certain methods presented in the paper.

Table 9: The spectral radii of the iteration matrix for the 1QSCB-CN method applied to problem (27)-(29).

σ	$N=8$	$N=16$	$N=32$	$N=64$	$N=128$	$N=256$
0.01	0.998459	0.999615	0.999904	0.999976	0.999994	0.999998
0.10	0.984697	0.996152	0.999037	0.999759	0.999940	0.999985
0.25	0.962177	0.990408	0.997593	0.999398	0.999849	0.999962
0.50	0.925758	0.980907	0.995192	0.998796	0.999699	0.999925
1.00	0.856831	0.962176	0.990408	0.997593	0.999398	0.999849
1.50	0.792667	0.943795	0.985646	0.996392	0.999097	0.999774
2.00	0.755162	0.925756	0.980907	0.995192	0.998796	0.999699
2.50	0.799213	0.908049	0.976191	0.993994	0.998495	0.999624
3.00	0.829830	0.890664	0.971497	0.992797	0.998194	0.999548
3.50	0.852346	0.873593	0.966826	0.991602	0.997894	0.999473
4.00	0.869599	0.868258	0.962176	0.990408	0.997593	0.999398
4.50	0.883242	0.882032	0.957548	0.989215	0.997293	0.999323
5.00	0.894301	0.893199	0.952942	0.988024	0.996993	0.999247
6.00	0.911135	0.910200	0.943795	0.985646	0.996392	0.999097
7.00	0.923343	0.922532	0.934734	0.983274	0.995792	0.998946
8.00	0.932602	0.931885	0.931838	0.980907	0.995192	0.998796
10.00	0.945716	0.945135	0.945096	0.976191	0.993994	0.998495
15.00	0.963480	0.963086	0.963059	0.964498	0.991005	0.997744
20.00	0.972485	0.972186	0.972166	0.972166	0.988024	0.996993

Table 10: The spectral radii of the iteration matrix for the 1QSC-CN method applied to problem (27)-(29).

σ	$N = 8$	$N = 16$	$N = 32$	$N = 64$	$N = 128$	$N = 256$
0.01	0.998459	0.999615	0.999904	0.999976	0.999994	0.999998
0.10	0.984698	0.996152	0.999037	0.999759	0.999940	0.999985
0.25	0.962178	0.990408	0.997593	0.999398	0.999849	0.999962
0.50	0.925760	0.980907	0.995192	0.998796	0.999699	0.999925
1.00	0.856835	0.962176	0.990408	0.997593	0.999398	0.999849
1.50	0.792673	0.943796	0.985646	0.996392	0.999097	0.999774
2.00	0.783209	0.925756	0.980907	0.995192	0.998796	0.999699
2.50	0.822724	0.908049	0.976191	0.993994	0.998495	0.999624
3.00	0.850055	0.890664	0.971497	0.992797	0.998194	0.999548
3.50	0.870084	0.873593	0.966826	0.991602	0.997894	0.999473
4.00	0.885393	0.884249	0.962176	0.990408	0.997593	0.999398
4.50	0.897475	0.896444	0.957548	0.989215	0.997293	0.999323
5.00	0.907252	0.906314	0.952942	0.988024	0.996993	0.999247
6.00	0.922108	0.921314	0.943795	0.985646	0.996392	0.999097
7.00	0.932862	0.932174	0.934734	0.983274	0.995792	0.998946
8.00	0.941006	0.940400	0.940396	0.980907	0.995192	0.998796
10.00	0.952525	0.952034	0.952031	0.976191	0.993994	0.998495
15.00	0.968098	0.967765	0.967763	0.967763	0.991005	0.997744
20.00	0.975977	0.975726	0.975724	0.975724	0.988024	0.996993

Table 11: The spectral radii of the iteration matrix for the QSC-CN0 method applied to problem (27)-(29).

σ	$N = 8$	$N = 16$	$N = 32$	$N = 64$	$N = 128$	$N = 256$
0.01	0.998459	0.999615	0.999904	0.999976	0.999994	0.999998
0.10	0.984696	0.996152	0.999037	0.999759	0.999940	0.999985
0.25	0.962177	0.990408	0.997593	0.999398	0.999849	0.999962
1.00	0.856880	0.962177	0.990408	0.997593	0.999398	0.999849
2.00	0.732987	0.925760	0.980908	0.995192	0.998796	0.999699
3.00	0.752437	0.890673	0.971497	0.992797	0.998194	0.999548
4.00	0.798876	0.856843	0.962176	0.990408	0.997593	0.999398
5.00	0.829066	0.829020	0.952943	0.988024	0.996993	0.999247
7.00	0.866711	0.866580	0.934735	0.983274	0.995792	0.998946
10.00	0.897957	0.897674	0.908050	0.976191	0.993994	0.998495
20.00	0.939210	0.939181	0.939181	0.952943	0.988024	0.996993
40.00	0.964553	0.963980	0.963978	0.963978	0.976191	0.993994